This document was prepared in conjunction with work accomplished under Contract No. DE-AC09-96SR18500 with the U. S. Department of Energy.

DISCLAIMER

FY2004 Corrosion Surveillance Results For L-Basin (U)

Philip R. Vormelker, Andrew J. Duncan, and Tracy H. Murphy

Savannah River National Laboratory
Materials Science and Technology

Publication Date: September 2005

Westinghouse Savannah River Company
Savannah River Site
Aiken, SC 29808

This document was prepared in connection with work done under Contract No. DE-AC09-96SR18500 with the U. S. Department of Energy

DISCLAIMER

DOCUMENT: WSRC-TR-2005-00067

TITLE: FY2004 Corrosion Surveillance Results for L-Basin (U)

MS&T APPROVALS

[redacted]

Date: _____

Philip R. Vormelker, Author
Materials Application and Process Technology Group
Materials Science and Technology

Date: _____

Andrew J. Duncan, Author
Materials Application and Process Technology Group
Materials Science and Technology

Date: _____

Tracy H. Murphy, Author
Materials Application and Process Technology Group
Materials Science and Technology

Date: _____

John I. Mickalonis, Technical Reviewer
Materials Science and Technology

Date: _____

R. L. Sindelar, Manager
Materials Application and Process Technology Group
Materials Science and Technology

Date: _____

N. C. Iyer, Director
Materials Science and Technology

DOCUMENT: WSRC-TR-2005-00067

TITLE: FY2004 Corrosion Surveillance Results for L-Basin (U)

CUSTOMER APPROVALS

[redacted]

_____ Date: _____
R. W. Deible, Engineer
SFP Operations Engineering
Operations Business Unit

_____ Date: _____
T. J. Spieker, Manager
SFP Operations Engineering
Operations Business Unit

TABLE OF CONTENTS

LIST OF TABLES

LIST OF FIGURES

Page

Page

LIST OF ABBREVIATIONS

DOE	Department of Energy
DRR	Domestic Research Reactor
FRR	Foreign Research Reactor
MS&T	Materials Science and Technology
PTFE	Polytetrafluoroethylene
RBOF	Receiving Basin for Offsite Fuel
SNF	Spent Nuclear Fuel
SRS	Savannah River Site
SRNL	Savannah River National Laboratory
SRTC	Savannah River Technology Center (previous name)
SS	Stainless Steel

1.0 Summary

This report documents the results of the L-Basin Corrosion Surveillance Program for the fiscal year 2004. Test coupons were removed from the basin on February 12, 2004, shipped to Savannah River National Laboratory (SRNL), and visually examined in a contaminated laboratory hood. Selected coupons were metallurgically characterized to establish the extent of general corrosion and pitting. Pitting was observed on galvanically coupled and on intentionally creviced coupons, thus demonstrating that localized concentration cells were formed during the exposure period. In these cases, the susceptibility to pitting was not attributed to aggressive basin water chemistry but to localized conditions (intentional crevices and galvanic coupling) that allowed the development of oxygen and/or metal ion concentration cells that produced locally aggressive waters. General oxidation was also observed on all of the coupons with localized corrosion observed on some of the coupons. These coupons were not pretreated to produce a protective oxide layer prior to exposure in the basin water. Non-protected coupons are more susceptible to corrosion than fuel cladding which has developed a protective oxide layer from high temperature reactor operations. However, the oxide on spent nuclear fuel (SNF) stored in L-Basin is not necessarily in pristine condition. Some of the oxide may have spalled off or been mechanically damaged prior to arrival at SRS. These areas on the fuel cladding would have the same susceptibility to corrosion as the coupons. Current observations from the test coupons demonstrate that, even with rigorously controlled basin water chemistry, localized aggressive conditions can develop in intentional crevice and galvanic samples. These results do illustrate the potential for corrosion induced degradation and thus the importance of a routine surveillance program similar to that conducted on the Uruguay fuel and on the surveillance coupons stored in L-Basin and future in-service inspections proposed for additional SNF in L-Basin.

The 2004 results are compared to previous results on coupons removed from SRS basins in fiscal years 2001, 2002 and 2003. The extent of corrosion is correlated with sample and storage conditions as well as the water chemistry during the storage period. Coupon weight gains from 2004 coupons are similar to those from 2003. Oxides were removed from furniture rack coupons from 2003 and 2004 and comparable pit depths were found in the filler metal.

Corrosion induced-degradation of the spent nuclear fuels stored in L-Basin could potentially impact the storage process by causing cladding penetration, exposing fuel core material, and allowing release of radionuclides to the basin waters. Such releases could potentially lead to high water activity levels which could impact fuel integrity and present problems in future fuel handling and transfer operations. However, the collective results (to date) of the coupon and water chemistry evaluations and Uruguay spent fuel inspections indicate that the fuel in the SRS storage basins has not experienced corrosion-induced degradation that will limit the time for interim storage in the basin waters. Continued surveillance and inspection is essential due to the potential for corrosion induced degradation. The next withdrawal of surveillance coupons from L-Basin occurred on March 29, 2005.

2.0 Introduction

Spent nuclear fuels from SRS nuclear materials production operations and the DOE-owned fuel used in foreign and domestic research and test reactors are now stored exclusively in the L-Basin. The production fuels were previously stored in K-, L-, P-Reactor basins and the research and test reactor fuels were primarily stored in the RBOF facility. L-Basin has now become the single SRS site for water storage of spent nuclear fuels.

The corrosion surveillance program, originally designed to monitor the condition of fuels stored in K-Basin, was initiated in 1992 and expanded to include L- and P-Basins and the RBOF facility in 1993. The surveillance of coupons and other test specimens and Uruguay fuel inspection allow early detection of corrosion mechanisms and assists in the evaluation of the potential for the L-Basin water to corrode the cladding materials on spent nuclear fuels. The P-, K- and RBOF-Basins were de-inventoried and surveillance programs were discontinued in 1996, 2002, and 2003, respectively. The L-Basin Corrosion Surveillance Program is continuing to demonstrate the resistance of the fuel claddings to corrosion in the basin water and to provide assurance of continued safe, interim storage.

Sets of standard corrosion coupons (70 mm and 32 mm diameter disks), including coupons representative of the aluminum cladding materials and storage rack materials used at SRS and in the research and test reactors, were placed in the SRS basins. Standard sets of coupons were developed through a cooperative, DOE complex wide assessment of basin corrosion and surveillance programs using the coupon sets that were initiated in 1995. The surveillance coupons were not pretreated to increase the thickness of the air formed, protective oxide before being placed in the basins. The use of an air-formed film was thought to provide a surface that is more susceptible to corrosion than the irradiated fuel cladding because high temperature reactor operations enhanced the protective quality of the oxide film.[1] The use of these non-irradiated coupons allows early detection of corrosion in advance of potential effects on fuel cladding and provides the opportunity to associate that corrosion with changes in the basin water chemistry. Aluminum alloy coupons of 1100, 5086, 6061, and 6063 (Table 1) were used to represent various fuel cladding and furniture rack alloys.

3.0 Procedure - Coupons

The FY2004 corrosion surveillance (circular disk) samples, removed from L-Basin on February 12, 2004, had been in wet storage since January 11, 1996, and thus had experienced more than 8 years immersion in L-Basin water. The furniture rack samples (flat plates, 6061-T6, and "U" channels, 6063-T5 with and without F4043 welds) were originally immersed in July 10-11, 1995. These samples experienced more than 9 years exposure in L-Basin water. Circular disk coupons (Figure 1) include individual alloys (with and without welds), galvanic couples between large 304 stainless steel (70 mm in diameter) disks and smaller aluminum disks (32 mm in diameter), and crevice coupons. All coupons were electrically isolated from the support rod with a Teflon®[1] (PTFE) washer. The coupons were removed from the storage racks and examined for evidence of pitting, galvanic attack, crevice corrosion and/or general corrosion. The observations on these samples are compared to those on surveillance coupons removed from the basins in FY2001, FY2002, and FY2003. The digital camera system, originally used in the FY2003 surveillance, has continued to allow a closer, more detailed examination of the coupons. The use of digital images allows brightness and contrast adjustments to enhance the photos used in this report. Since original lighting and camera angles were not always the same, some of the images may differ when comparing the same sample type. After the initial examinations, coupons with heavy oxide buildup and/or indications of localized corrosion were selected for nitric acid cleaning, metallographic examination, and pit analysis. Metallographic examinations focused on determining the extent of metal loss to general corrosion and characterizing local corrosion processes (galvanic, crevice and/or pitting corrosion). Pitting was evaluated per ASTM Specification G-46 [2] to determine maximum and average pit depths and pit density.

[1] Teflon is a registered trademark of DuPont

4.0 Corrosion Evaluation for L-Basin

The routine surveillance of corrosion samples, spent nuclear fuels and storage systems in L-Basin demonstrates that corrosion of the aluminum and stainless steel systems and components is successfully mitigated by water quality control. However, cervices and/or galvanic coupling coupons combined with isolated aggressive ion concentrations in the basin water have allowed localized corrosion processes to initiate in a few corrosion coupons. Past observations of galvanic corrosion between aluminum and stainless led to the removal of stainless steel hangers from the basins. The following subsections of this report discuss observations from coupons removed from L-Basin and use those observations to conclude that significant corrosion-induced degradation of spent nuclear fuels stored in L-Basin is unlikely. However, the presence of incipient, localized corrosion in coupons (crevice and galvanic) emphasizes the importance of water quality control and surveillance to assure that the interim storage conditions in L-Basin continue to inhibit corrosion induced degradation in stored spent nuclear fuel.

4.1 Corrosion Evaluation

4.1.1. Water Quality

L-Basin was chosen to receive domestic and FRR fuel because it had greater capacity and was in better physical condition than the other reactor basins.[3] Previous to July 1995 a portable deionizer was rotated among C-, K-, L-, and P-Reactor basins to control basin chemistry. A temporary deionizer was installed in L-Basin in mid 1995 when the basin had an initial conductivity of approximately 100 µS/cm.[3] By the end of October 1995, conductivity values decreased to 3 µS/cm and below. Concentrations of Cl^- were also substantially reduced. A dedicated deionizer system was placed into service in June 1996 to maintain the high water quality.

The overall water quality in L-Basin has been maintained within Chemistry Program limits as shown in Figure 2 and Figure 3, where pH and conductivity of the water are shown as a function of time. Conductivity and pH remained within limits (< 10 µS/cm and 5.5 – 8.5, respectively [4]) during the period up to February 2004 throughout the evaluation period. This period corresponds to the time that the surveillance samples examined in this evaluation were stored in L-Basin. It appears that conductivity is leveling off at approximately 0.5 µS/cm while pH is leveling off at 6 as shown in Figure 3.

Figure 4 shows that increases in Cs-137 activity levels did not affect pH and conductivity levels over the time period from late 2002 to early 2004 when the samples were removed. The spike in Cs-137 levels was due to transfer of SNF to L-Basin. SNF transfer normally involves changing fuel bundles from the vertical to the horizontal position at which time leakage of Cs-137 occurs. Since conductivity increases would normally allow increased electron flow with expected increases in corrosion, the independence of radiation levels, at least from Cs-137, suggest that corrosion processes are not affected by increases in Cs-137 activity levels.

Figure 5 indicates the level of aggressive ion (Cl^-, Cu^+, and Hg^{+2}) concentrations over the same period but reveals that Cl^- concentration was slightly above target values during December-January 1999. During the October 2002-March 2004 period shown in Figure 6, Cl^-, Cu^+, and Hg^{+2} were at or below their respective program limits, 0.1 ppm for Cl^- and Cu^+ and 0.014 ppm for Hg^{+2}.

The current water chemistry results indicate that the on-line deionizer is working very well. Oxide formation on the surveillance coupons was typically uniform with corrosion at extremely low rates. This reinforces the current position that the present water chemistry controls are sufficiently conservative to mitigate corrosion in the basins, with the single exception that the onset of localized corrosion processes was observed in intentionally creviced and/or galvanically coupled corrosion coupons.

4.1.2. Evaluation of Corrosion Specimens

Selected images of individual 2004 surveillance coupons are shown in Figure 7. Percentage weight gains of approximately 0.85-1.05 % for the 2004 aluminum samples versus weight gains of 0.4 to 1.15% for 2003 are graphed in Figure 8. The welded coupons gained slightly more than the non-welded coupons in 2003 but this was not repeated in the 2004 coupons. One welded 6061 coupon from 2004 revealed percentage weight gains equal to or slightly less than the gains of the non-welded 6061 coupons. This is unusual since the autogeneous weld is expected to show more corrosion based on the 2003 data. One of the 1100 coupons (2003) did show a lower percentage weight gain due to slightly higher initial weight and slightly lower weight gain (± 0.5 gram) which was not repeated by the 2004 coupon results. Overall, these coupons appear visually comparable to coupons withdrawn in 2001, 2002, and 2003. The individual coupons from all four years of evaluation appear to be undergoing uniform oxidation.

The most appreciable oxide buildup observed is in galvanic couples, which is marked by heavy oxidation between the samples of dissimilar metals (see Figure 9 to Figure 11). Howell [5] and Vormelker [6] noted similar behavior in 2001 and 2003, respectively. The coupons from the years 2001 to 2003 appear similar. Selected galvanic coupons from 2004, representing the different aluminum alloys in contact with 304, were photographed and then cleaned with a 16M nitric acid solution (approximately 1.5 hours) for oxide removal.[7] Multiple (stirred) immersions were performed with weights measured before and after each cleaning step to ensure oxide removal and not the removal of metal. Small amounts of oxide remained on a few coupons. The effect on pit depth measurements is estimated to be less than 0.0005 inch. Aluminum (1100 and 6061) galvanic coupons are shown in Figure 10 with no visible pitting in the cleaned coupons. However, Figure 11 does reveal pitting in the cleaned 6063 coupon within the surface area mated to the stainless coupon and at the edges of the PTFE washer. Multiple pit sites were also observed on the 6063 coupon in the 2003 corrosion surveillance report.[6] Galvanic corrosion (pitting) is expected on aluminum/stainless steel combinations since aluminum is anodic to stainless steel. Pitting beneath the edge of the PTFE washer is due to crevices that exist between the surfaces of the two materials. Pitting on the 6063 coupon could also be due to end grain attack since the coupons were cut from an extruded bar. Thus, the face of the 6063 coupon represents the end of the bar and is subject to end grain attack.

Normalized weight gains of aluminum alloy couples are shown in Figure 12. The weights were normalized by dividing by the exposed surface area of each coupon. Prior to installation in L-Basin, the samples, purchased with a 120 grit finish, displayed a uniform, clean surface with no oxidation. In all cases the smaller coupon (32 mm diameter) displayed more weight gain than the larger coupon (70 mm diameter), regardless of the alloy combination. The higher normalized weight gain values of the 32 mm coupons is due to the smaller surface area exposed to the L-Basin water versus the larger surface areas of the 70 mm coupons. The combination of galvanic and crevice corrosion caused higher corrosion levels on the smaller coupled coupons. Thus, if aluminum SNF were hanging from stainless steel hangers connected to a stainless steel rack, galvanic corrosion could be a problem. However, by keeping the area of the cathode (stainless steel) small compared to the larger anode (aluminum), galvanic corrosion would be minimized. Galvanic connections with aluminum SNF have been removed

from L-Basin due to past corrosion problems. Galvanic couples do exist between stainless steel/zircaloy clad fuels and aluminum cans, and between stainless steel cans and aluminum cans.[8] However, the contact area is small (limiting anode to cathode area ratios) which should limit corrosion and its effects on can structural integrity.

Pit depths were measured on all 2004 galvanically coupled aluminum alloy coupons and summarized in Figure 13 with a display of average and maximum pit depths. Only selected coupons from the 2003 surveillance were measured and reported. Within each two alloy groupings in Figure 13, the diameter of the specimen on the left is 32 mm and that of the specimen on the right is 70 mm. The size difference is intentional in order to accelerate pitting rates from galvanic corrosion in the smaller specimen. The highest average (~6 mils) and maximum (8.5 mils) pit depths were revealed on the 6063 coupon which was coupled with 304. These pits are probably due to a combination of galvanic corrosion and end grain effects. Similar effects were also displayed on the 6063/304 coupled coupon from 2003. Maximum pit depths on the aluminum alloy couples were located near the PTFE washer circumference and on the ID and OD of the samples. This is also an indication that crevice corrosion is ongoing beneath the PTFE washer.

Figure 14 displays pit depth data from selected coupons shown from previous surveillance (FY2003) which shows the greatest average (17 mils) and maximum pit (23 mils) depths in the 6063 coupon mated to 304. These values are more than twice that of a similar galvanic coupon from 2004. For all samples, average pit depths were taken from the 10 deepest pits per ASTM G46.[2] From the previous data shown in Figure 14, it is evident that average and maximum pit depths are observed to be deepest in specimens coupled with 304 (stainless steel). This is expected since aluminum is highly anodic to stainless steel based on the galvanic series.[9] In addition, the pit depth values in an uncoupled 1100 coupon and a crevice 1100W (welded) coupon were observed to be elevated in comparison to the other coupons (7-8 mils average and 13 mils maximum depth for one uncoupled 1100 coupon and 4 mils average and 7-8 mils maximum depth for a welded 1100 coupon with the PTFE crevice washer). In comparison, pit depths in the second uncoupled 1100 coupon averaged less than 2 mils with a maximum pit depth less than 4 mils. Since the sample size is limited to two coupons, conclusions about the variability of the data are limited and any statistical conclusion is invalid.

Pit growth rates for 2004 are shown in Figure 15 which reveals average and maximum growth rates for the 2004 galvanically coupled coupons. In all but one coupon set, the average growth rate is less than 0.4 mils per year (mpy). The 6063 coupon mated to 304 reveals the highest average growth rate (approximately 0.7 mpy) that is approximately 2x that of the other coupons. In Figure 14, a similar 6063 coupon mated to 304 revealed an average growth rate of < 3 mpy. The average growth rates calculated for the 2003 coupons are below 3 mpy versus 0.7 mpy for the 2004 galvanic coupons. Pit growth rate may be slowing down.

The 6063 coupons are further examples of pit depths altered by the grain morphology. It appears that end grain attack present in the surface of the 6063 and at the edges of 1100 specimens has affected the data in Figures 13, 14, 15 and 22. End grain attack may play a role in corrosion at the rolled ends of spent fuel cladding fabricated into flat plates. However, the fuel meat region is sufficiently distant from the affected ends so that the fuel should remain protected. Also, SNF tends to be heavily oxidized due to high temperature reactor operation which should preclude the base metal from basin exposure. In cases where the oxides on SNF cladding have been damaged, the cladding would be exposed to the water chemistry with a possibility of end grain attack and pitting. To date, visual inspection of the Uruguay fuel in L-Basin wet storage has not revealed end grain attack, pitting, or other degradation in the expected end grain areas.[10]

A PTFE crevice washer with serrated edges was used on one side of a few 1100 and 6061 coupons. These coupons are shown in Figure 16 and Figure 17 with no visible pitting and the imprint of the serrated washer is still visible after 1.5 hours of nitric acid cleaning. Autogeneous welded 1100 and 6061 coupons are shown with and without a crevice washer in Figure 18 to Figure 21. Although some oxide remains after cleaning, potential pits are revealed by black spots in the circumference area of the PTFE washer and within the autogeneous weld areas. The effect of the remaining oxide (indicated by black spots) on pit depth measurements was estimated to be less than 0.0005 inch. In Figures 15 to 20, yellow-orange spots show up in the color images in only one side of the coupons. This is suspected to be staining from L-Basin water because only the top surface of the coupon reveals this phenomenon.

Figure 22 shows the pit depth measurements for all welded and non-welded single and crevice coupons removed from the basin in 2004. The number of examined coupons was increased over the selection made on the 2003 surveillance coupons. As mentioned above, average pit depths were taken from the 10 deepest pits per ASTM G46 (averages calculated where <10 pits were found are denoted by an asterisk (*). Single 1100 and 1100W specimens exhibit larger pit depths than other alloys, an average pit depth of approximately 9 mils and maximum pit depth of approximately 14 mils for a single, uncoupled 1100 coupon. These pit depths are very similar to those displayed in Figure 14. As mentioned earlier for 1100 coupons, the deepest pits measured in these specimens were observed on or near the edges of the coupon. These pits are deeper as a result of their proximity to the end grains at the edge. In all single welded coupons, the weld metal contained higher average pit depths than the base metal. The same conclusion was not deduced from the welded crevice coupons. Low average pit depths of less than 3 mils were found in the weld and base metal in most of the welded coupons with a crevice washer. This implies that the PTFE crevice washer did not cause sufficient crevice conditions to increase corrosion. The lack of crevice corrosion under the crevice washer is probably due to the lack of sufficient spacing between the washer and the aluminum coupon. However, crevice corrosion was found on various corrosion coupons at the edges of the flat PTFE insulating washers which were installed on at least one side of most coupons in this study. The flat washer apparently creates greater surface area and/or volume in contact with the coupon for potential crevice corrosion.

Pit density measurements were also measured for a selected number of autogenously welded and filler metal welded rack coupons. Pit densities were not measured on non-welded individual, crevice, and galvanic coupons because the number of pits within a 0.762 mm square area was less than that measured for the welded coupons. Pit density is determined by the number of pits measured within a 0.762 mm (0.030 inch) square area. The pit data from autogeneous welded disk coupons of 1100 and 6061 are shown in Figure 23 along with pit density measurements from rack coupons containing fillet welds of R4043 in Figure 24. Figure 23 clearly shows higher average (≤ 65 pits/mm^2) and maximum (≤ 90 pits/mm^2) pit densities in the autogeneous welded disk coupons (with and without crevice washer) versus the filler metal welded furniture rack samples (≤ 15 pits/mm^2). This is most likely to be a result of the thermal profile of the autogenous weld promoting pit growth due to changes in the metallurgical microstructure (grain growth, dissolution or growth of intermetallic phases) versus the normal weld microstructure of the filler metal (R4043) used on the rack coupons.

The as-received condition of the aluminum support rack coupons after L-Basin exposure, both welded and non-welded, is shown in Figure 24. These aluminum rack furniture samples, with and without welds, were immersed in L-Basin for approximately 97 months. Corrosion is visible as the white oxide formation in the heat affected zone (HAZ) of the welds with no apparent visual differences between the 2004 rack coupons and those from previous years. The visual appearance does not indicate a substantial increase in degradation. Examination of the weld HAZ in a scanning electron microscope revealed rod-type morphology versus round particles

found on the base metal (6063 T5) as shown in Figure 25. Analysis of the HAZ (spot 10) by electron dispersive spectroscopy (EDS) revealed the presence of zinc. Specific Zn levels were not measured since this particular contaminated EDS system is not equipped for quantitative analysis. The chemical composition of the 6063 base metal and the R4043 in Table 1 shows that zinc levels are at or below 0.10%. Zinc levels in 6061 are more than double that of 6063 and the oxides may show this same behavior. Even though the 0.10% level in 6063 is below the detectible limit of EDS analysis (≥ 0.20%), zinc was detected in the surface oxides in the weld HAZ in 6063. A recent chemical analysis of L-Basin water revealed a zinc level of 0.17 ppm. These levels are extremely low and thus conclude that Zn absorption from L-Basin water is probably not causing the presence of Zn in the surface oxides. Another source of Zn may also be from preferential oxidation of zinc from the sample. Zinc is normally anodic to aluminum. This has to be further explored in future work.

An original 6063 furniture rack U-channel weld is shown in Figure 26. This original welded coupon, provided by the manufacturer of the fuel rack installed in L-Basin, shows evidence of being etched or bead blasted (Figure 26.) which probably matches the condition of the furniture rack coupons installed in L-Basin. After nitric acid cleaning of the welded coupons was performed per Reference 7, numerous pitting sites were exposed in the weld metal (Figure 27 to Figure 28) on both the 6061 plate and the 6063 U-channel. Pit depths ranged from a less than 0.5 mils in the base metal to a maximum of 6 mils in the toe of a welded plate (Figure 29) with average pit densities ranging from 2 to 16 pits/mm^2 (Figure 29). The maximum pit density, 16 pits/mm^2, was in the weld of a 6061 T6 plate from 2003. This value is much higher than the other welded plate coupon in which the maximum pit density was approximately 5 pits/mm^2. The maximum pit density in the two U-channel coupons is less than 10 pits/mm^2. Although initially thought to be the result of a galvanic reaction between the base and weld metal, referenced electrode potentials of 6061, 6063, and R4043 in a NaCl-H_2O_2 solution are -0.80 to -0.83 volts.[11] These potentials are virtually the same and thus a galvanic reaction should not occur between the weld and the base metals in this unique solution. Although the application of R4043 is normal industry practice as a corrosion resistant filler metal for both 6061 and 6063, the electrode potentials of the three alloys need to be measured in solutions similar to L-Basin.

5.0 Conclusions

The results for the FY2004 corrosion surveillance specimens yielded similar observations to those found in previous years, for the storage conditions that existed during immersion (January 1996 through February 2004). Pitting in the rack coupons was not investigated prior to this evaluation. Both conductivity and pH levels appear to be leveling off at 0.5 µS/cm and 6, respectively which are well below the specified Chemistry Program limits (< 10 µS/cm and 5.5 – 8.5, respectively). Cl^-, Cu^+, and Hg^{+2} concentrations are below their respective limits, 0.1 ppm and 0.014 ppm (Hg^{+2}). The water chemistry is indicative of extremely pure water which should minimize corrosion in these coupons and the spent fuel in the basin.

The following are concluded based on the FY 2004 coupon surveillance:

- Uniform surface corrosion was observed on most surveillance coupons.
- No significant difference in corrosion performance was observed among the aluminum alloy corrosion surveillance disk coupons (i.e., 1100, 6061 and 6063). It appears that oxide growth was initially high and has grown at a much slower rate or has stabilized.
- Although no apparent visual differences in performance was observed between galvanic couples and crevice corrosion specimens removed in FY2003, and FY2002, in-depth

cleaning and evaluation was performed on the FY2003 and the FY2004 coupons. This improved technique (along with digital photographic technology) revealed pitting in the galvanic and crevice coupons. Although, not noted in previous years' inspections, pitting of this type would not be visible without cleaning and evaluation (a process not performed previously). This occurs even in the basin with excellent water chemistry due to the localized conditions (galvanic corrosion and crevices between mating coupons and washers) in these samples.

- Selected coupons revealed pitting in various areas, including ID and OD circumferences (due to end grain attack), autogeneous welds, and beneath the PTFE insulating washer. This was similar to the conclusions reported on the 2003 coupons. The pit density in the welded coupons was significantly higher than the rest of the coupons.

- Some differences were noted between average and maximum pit depths of the same type coupon. This is probably due to the small number of evaluated coupons, a non statistical sample.

- Pit depths in the 2004 coupons are lower than those from 2003. Subsequently, pit growth rates for 2004 coupons are also lower due to an additional year of exposure. While the 2004 coupons are from the same heat of material as the 2003 coupons there may be microstructural differences between the coupons which would allow pitting variances.

- Weld specimens from rack furniture samples from 2003 and 2004 show evidence of oxide buildup with multiple pitting sites revealed below the oxide on the weld metal and at the weld toe. The pitting observation is new compared to past analysis of the furniture rack samples. It is expected that previous rack samples removed from the basin were also pitted. The effect of pitting in the welded rack metal should be further investigated, if accessible, during the future fuel inspection program. Also, the long term effect of weld pitting on the structural integrity of the fuel racks should be examined.

6.0 Recommended Path Forward

For 2005, the following is recommended:

- The next set of coupons to be analyzed will be a junior ray gun which contains a reduced number of coupons compared with the coupon sets removed prior to 2005. They were installed on May 15, 1995 and one set was removed on March 29, 2005. The coupons are in the process of evaluation.
- With the discovery of pitting in the welds on the furniture rack coupons, the electrode potentials of welded plate and U-channel coupons in L-Basin water or its equivalent need to be evaluated to determine if there are galvanic effects between the weld and base metals. Also the long term effect of pitting on the structural integrity of the welded fuel racks should be investigated. The inspection of fuel rack welds should be considered.
- Continued inspection and evaluation of the Uruguayan RU-1 nuclear fuel is recommended to provide data and verification of the effectiveness of the basin chemistry control program and to provide information on the consequences of dry storage of spent fuel versus wet storage. This program currently includes biennial inspection of four RU-1 assemblies in K assembly area dry storage and annual inspection of four wet-stored

RU-1 assemblies in L-disassembly basin. The results of the 2004 inspection are being summarized into a Technical Report.

7.0 References

1. G. T. Chandler, R. L. Sindelar, and P. S. Lam, "Evaluation of Water Chemistry on the Pitting Susceptibility of Aluminum," Corrosion/97, Paper No. 104, (Houston, TX: NACE International, 1997).
2. ASTM G-46, "Standard Guide for Examination and Evaluation of Pitting Corrosion," American Society for Testing and Materials (1999).
3. J. P. Howell, "Corrosion Surveillance Program for Foreign Research Reactor Fuel in L-Reactor Disassembly Basin (U)," Interoffice Memorandum SRT-MTS-94-0170, January 11, 1995.
4. D. C. Mercado, "Basin Water Chemistry Control Program," Technical Report No. WSRC-TR-97-0239, Rev. 4, September 2004.
5. J. P. Howell and D. W. Vinson, "Basin Corrosion Surveillance Evaluation-CY2001," Technical Memorandum SRT-MTS-2001-20021, July 2001.
6. P. R. Vormelker, A. J. Duncan, and D. W. Vinson, "FY2002/FY2003 Corrosion Surveillance Results for the SRS Basins (U)," Technical Report WSRC-TR-2003-00548, December 2003.
7. R. S. Ferrer and R. G. Kelly, Corrosion 57, 2 (2001), p. 110-117.
8. R. W. Deible, "Spent Fuel Isolation Cans Inventory," M-TRT-L-00003, March 22, 2005.
9. ASM Handbook Ninth Edition, *Volume 13 Corrosion*, "Evaluation of Galvanic Corrosion," J. E. Davis Ed, ASM International (September 1987), p 235.
10. P. R. Vormelker and D. W. Vinson, "Inspection of Wet Uruguay Spent Fuel from L-Basin (U)," Technical Report WSRC-TR-2005-00216, to be issued.
11. Corrosion of Welded, Brazed, Soldered, and Adhesive-Bonded Joints, *Corrosion of Aluminum and Aluminum Alloys*, J. R. Davis, Ed., ASM International, 1999, pp. 161-169.

Table 1. Composition of Aluminum Surveillance Coupon Alloys

Aluminum Alloy Designation	Maximum Elemental Composition, %					
	Si	Cu	Mn	Mg	Zn	Other
1100	---	0.20	0.05	0.05	0.10	1.0 Max (Si + Fe)
5086	0.40	0.5	4.0	0.4	0.25	0.50 Fe/0.25 Cr
6061	0.8	0.40	0.15	1.2	0.25	0.35 Cr
6063	0.6	0.10	0.10	0.9	0.10	0.35 Fe/0.10 Cr
*R4043	6.0	0.30	0.05	0.05	0.10	0.8 Fe

* Welding rod for furniture rack samples

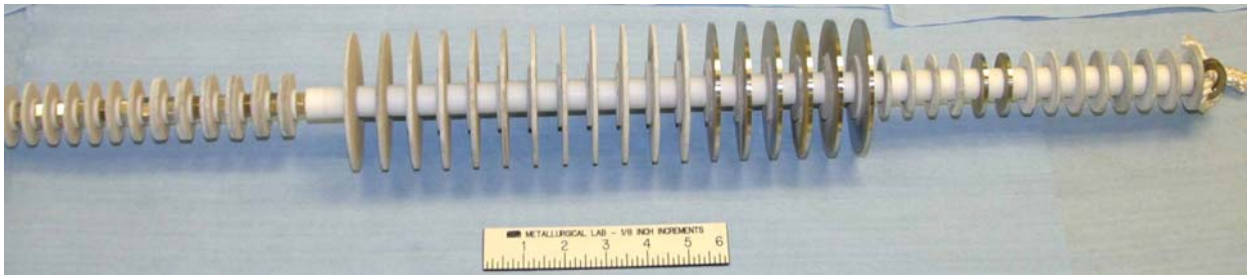

Figure 1. Disk coupons were removed on February 14, 2004 after 97 months immersion and are shown as-received from L-Basin on original hanging stainless steel rod.

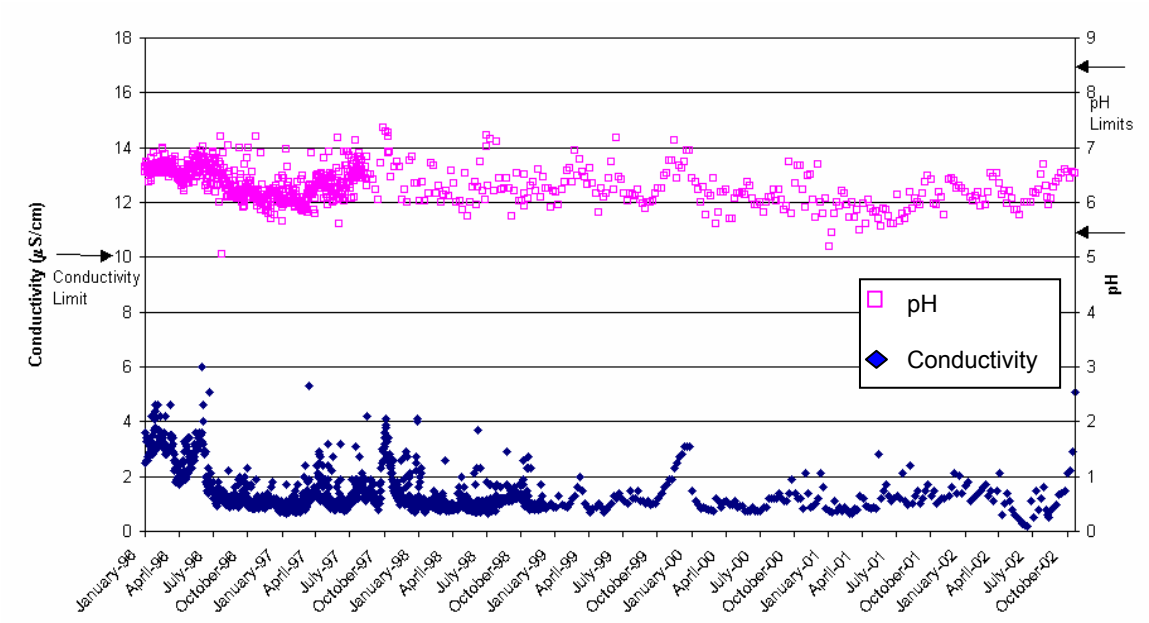

Figure 2. Time dependent water conductivity and pH in L-Basin during surveillance coupon immersion from January 1996 until October 2002.

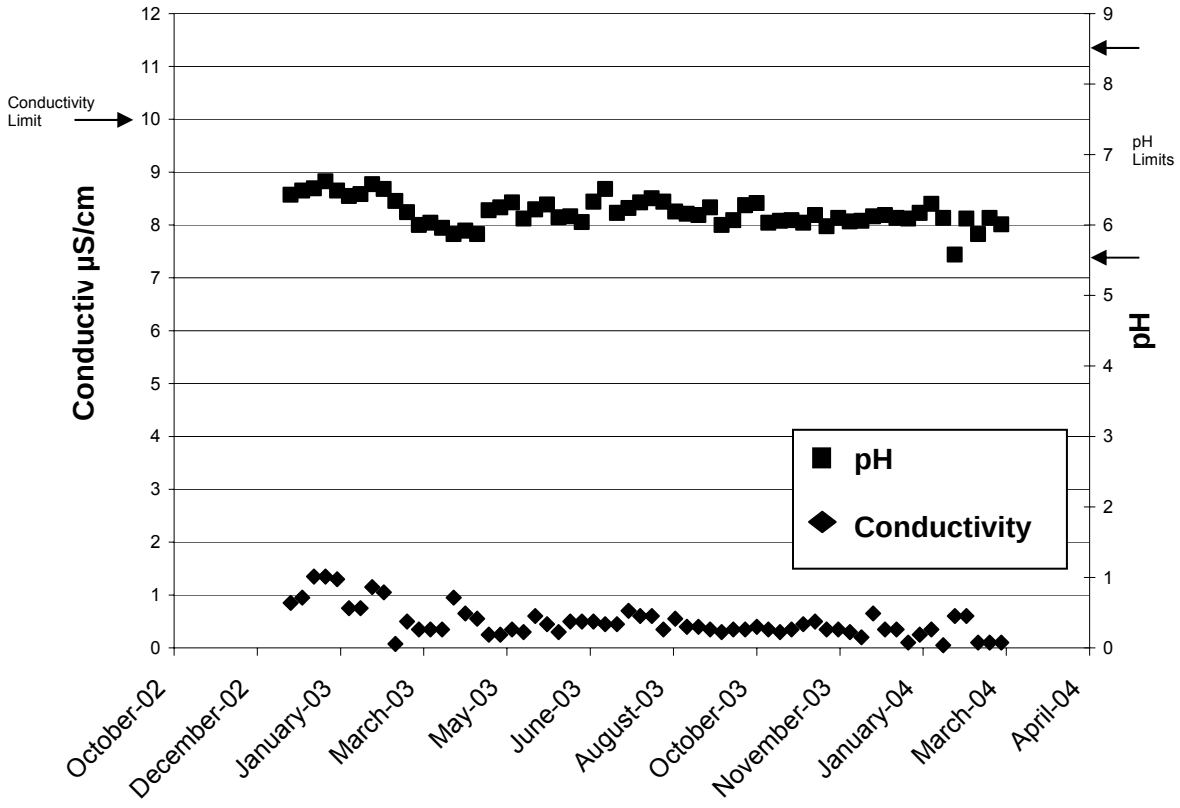

Figure 3. Time dependent L-Basin conductivity and pH from January 2003 until March 2004.

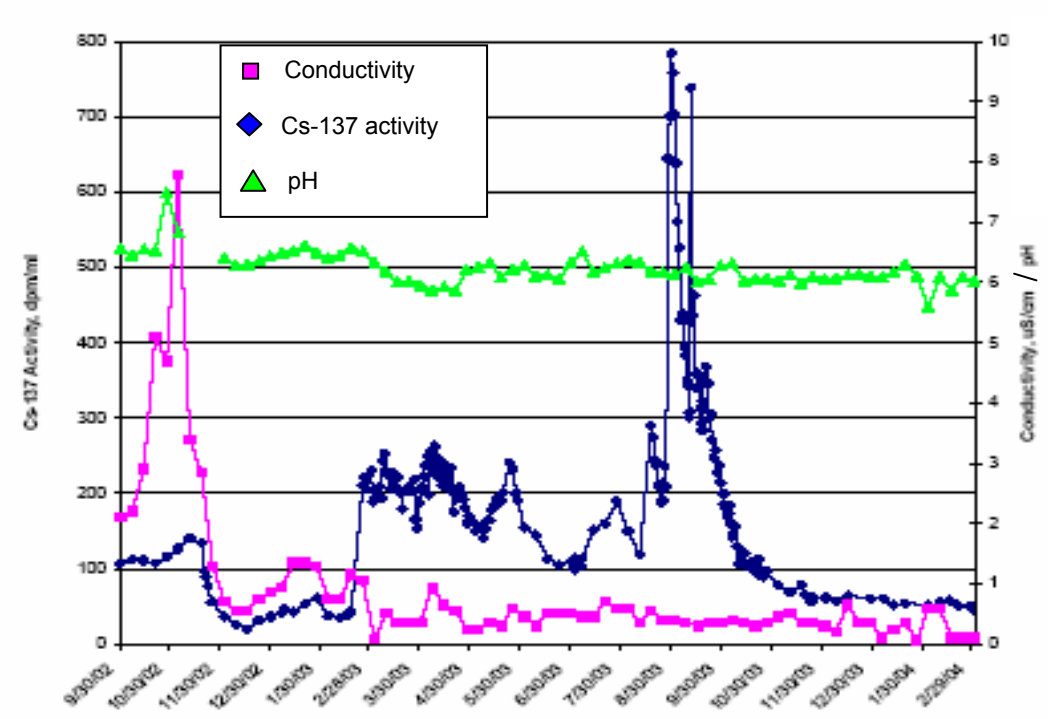

Figure 4. Time dependent Cs-137 activity levels in L-Basin versus pH and conductivity during October 2002 to the end of February 2004.

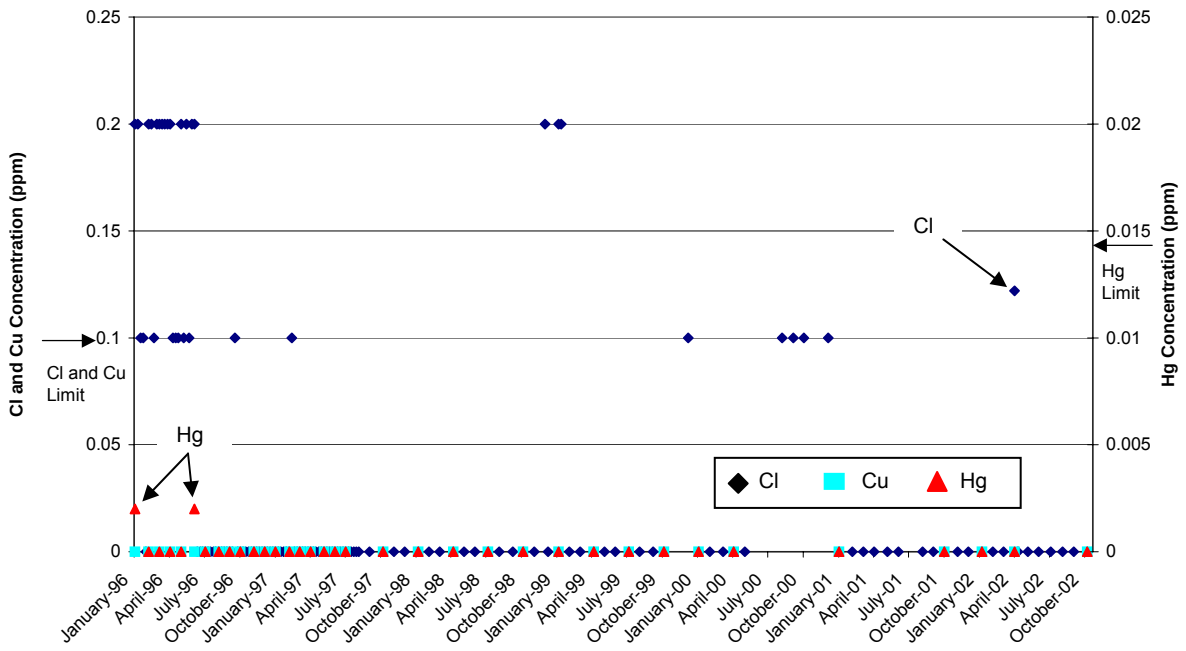

Figure 5. Time dependent concentration of aggressive species in L-Basin water during surveillance coupon immersion until October 2002.

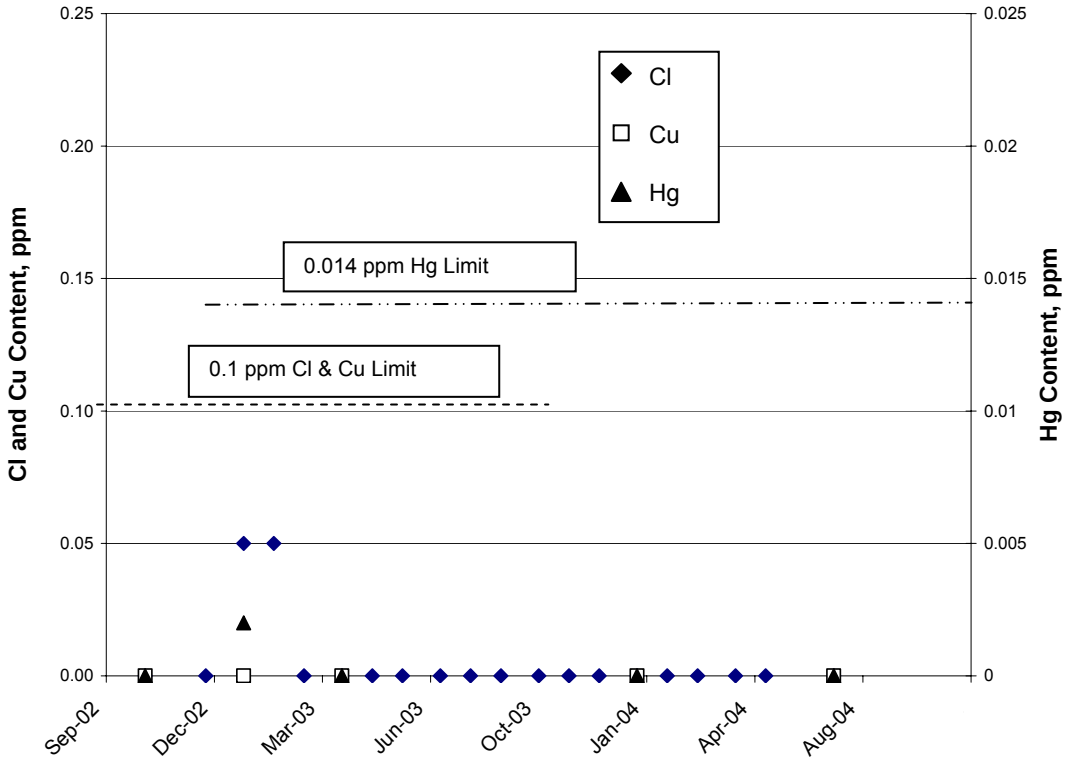

Figure 6. Time dependent concentration of aggressive species in L-Basin water during surveillance coupon immersion from October 2002 until July 2004. All species were below Chemistry Program limits.

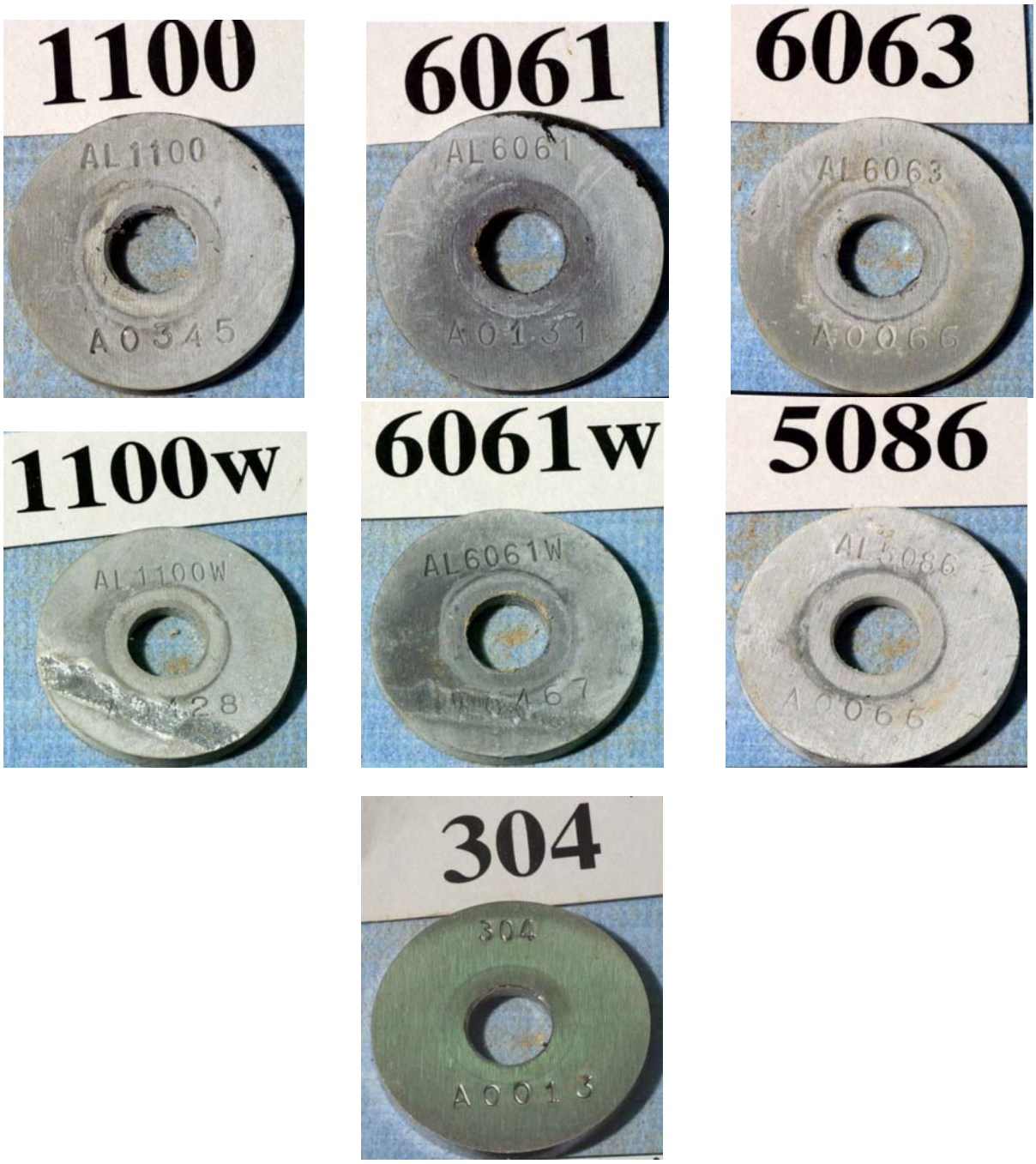

Digital Images

Figure 7. Examples of the individual coupons removed in 2004. Oxide scale in the PTFE washer area is visible in all, except for the 304. The amount of oxide growth appears to be minimal since sample identification is visible on all coupons shown above.

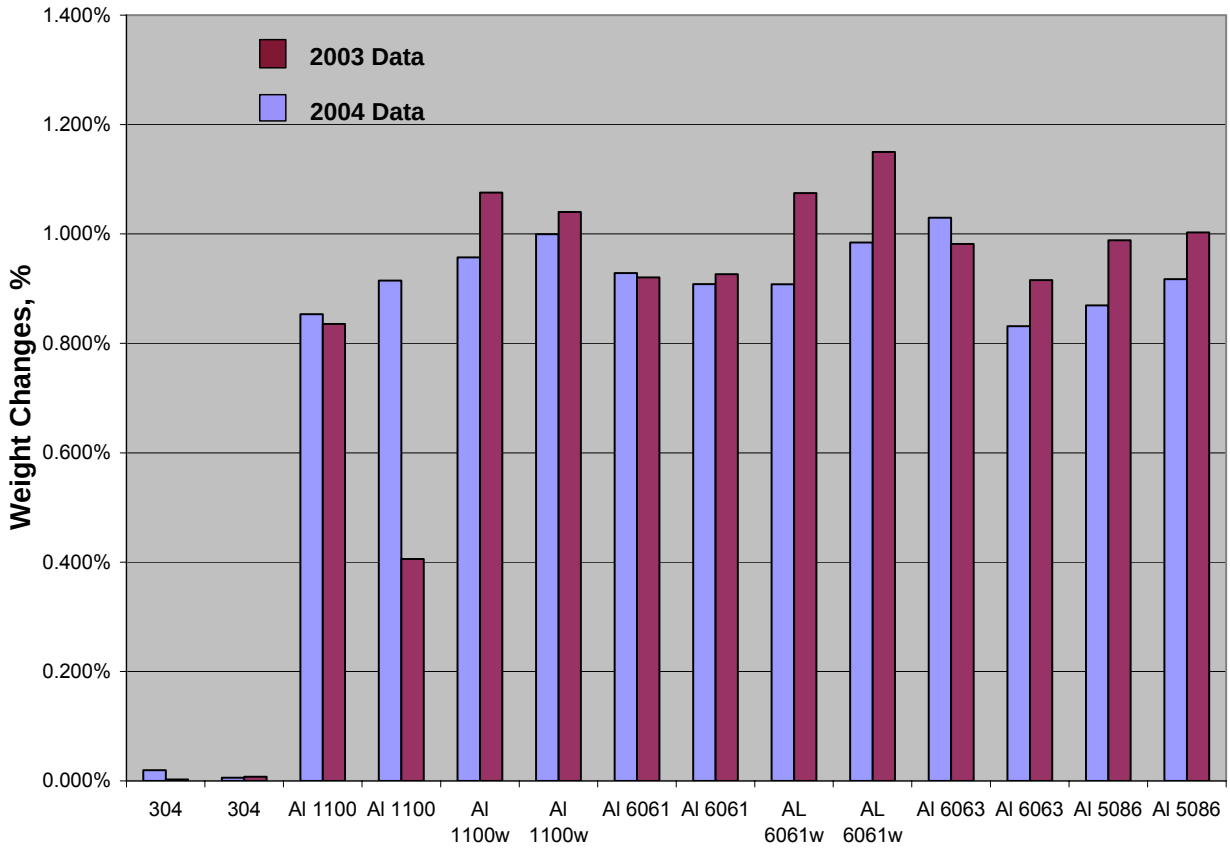

Figure 8. Percentage weight gains (weight gain divided by original weight x 100) from individual metal coupons from 2004 compared with those of 2003. In most cases, the coupons from 2003 appeared to gain a slightly higher percentage of their original weight. Note that the weight gains of welded samples in 2004 (alloy designation plus "w") were equal to or slightly more than their non-welded counterparts. The weight gain percentages of welded samples from 2003 were also higher than the non-welded samples.

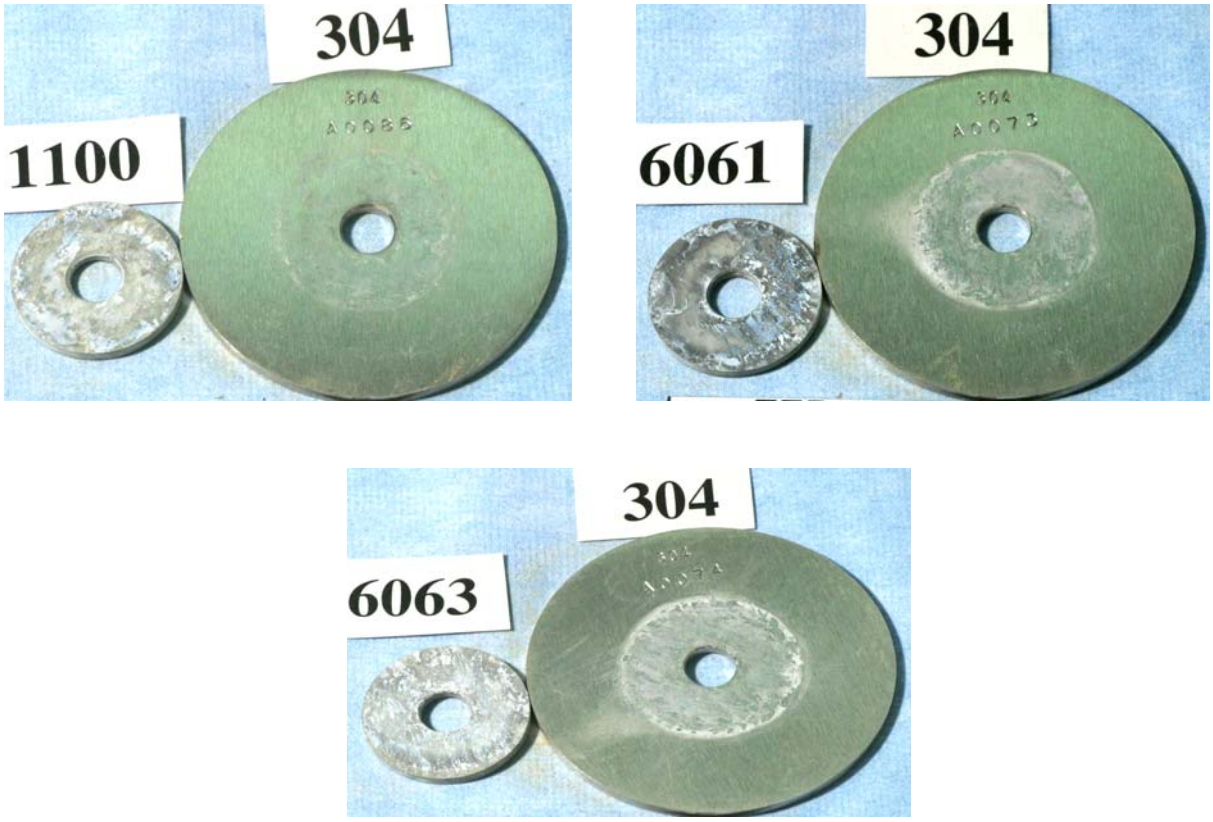

Digital Images

Figure 9. Aluminum 1100, 6061, and 6063 coupons galvanically coupled with 304 stainless steel are shown with mating surfaces in view. The surface characteristics of these mating surfaces after 8 years immersion remain similar to previously removed coupons.

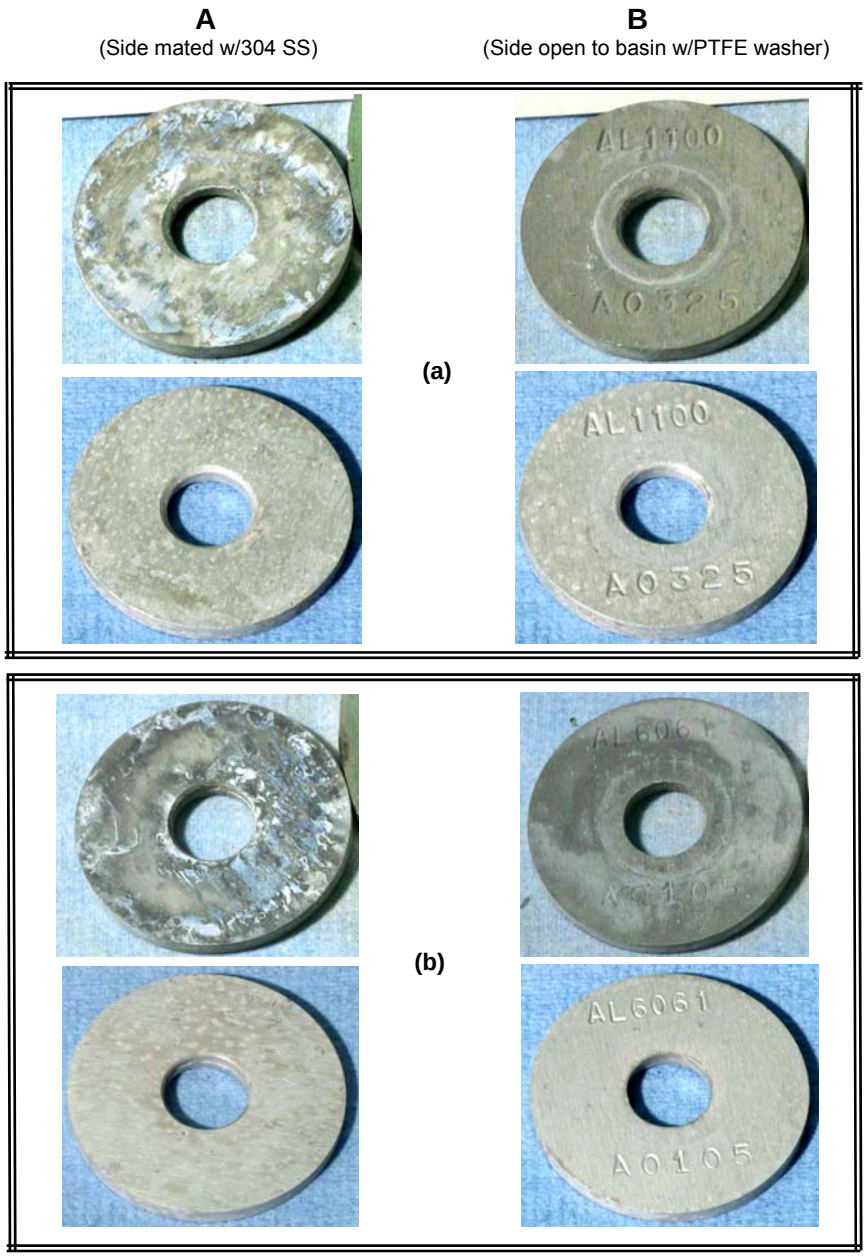

Digital Images

Figure 10. Before cleaning (upper photos in (a) box) and after cleaning (lower photos in (b) box) photos of selected aluminum galvanic coupons (32 mm OD) mated with larger (70 mm OD) 304 stainless steel coupons. Upper coupon group (a) is 1100 aluminum. Lower group is 6061 aluminum. Pitting is not visible in these images.

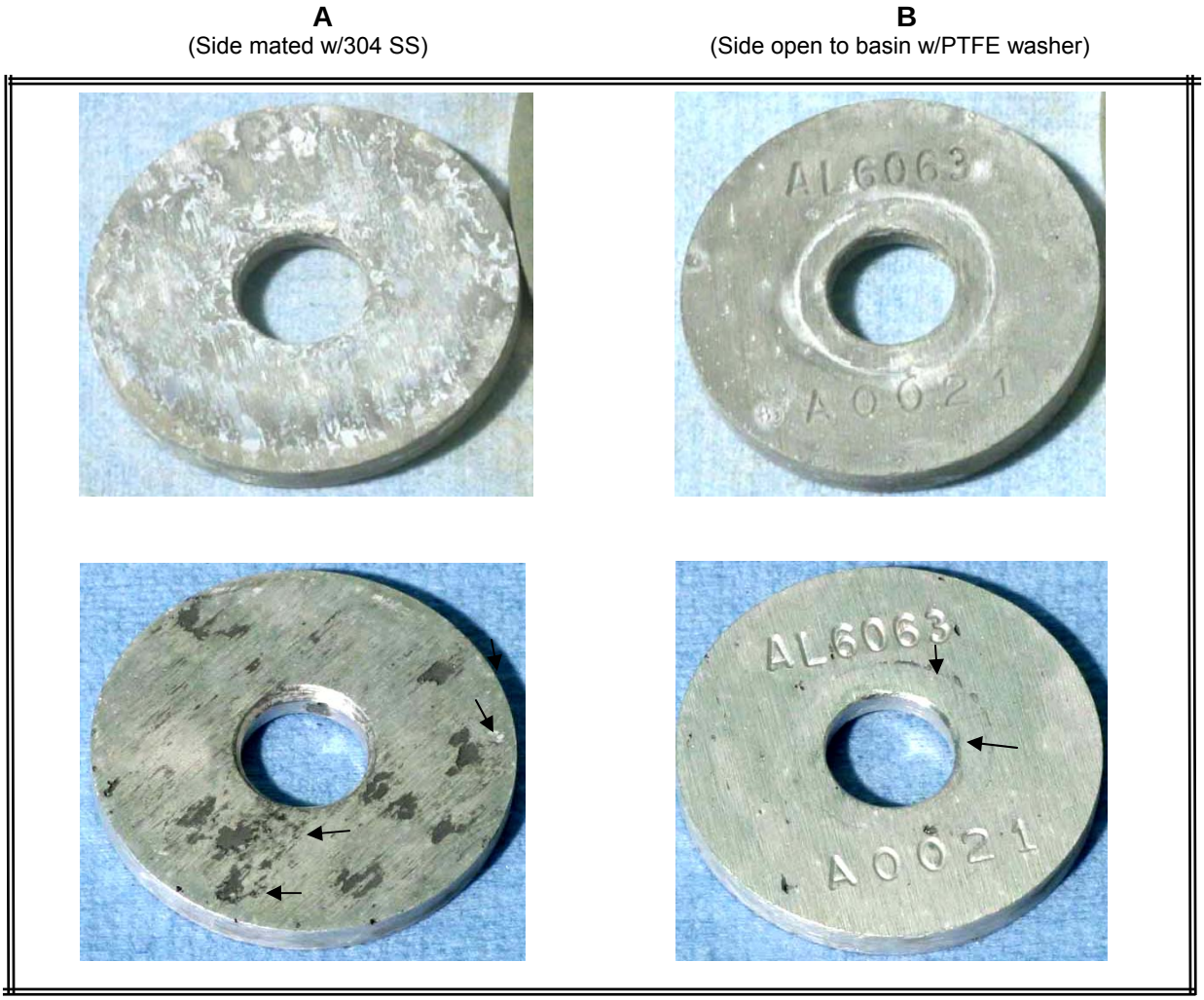

Digital Images

Figure 11. Aluminum 6063 coupon is shown before (upper) and after (lower) cleaning. Dark areas show remaining oxide that was not removed. Remaining oxide thickness on coupons is approximately 0.0005 inch which should not affect depth measurements. Pitting (noted by arrows) is visible in area that was beneath PTFE washer (lower right photo) and on coupon face (lower left photo) where crevice existed while in contact with 304 stainless steel. Original coupon diameter is 32 mm.

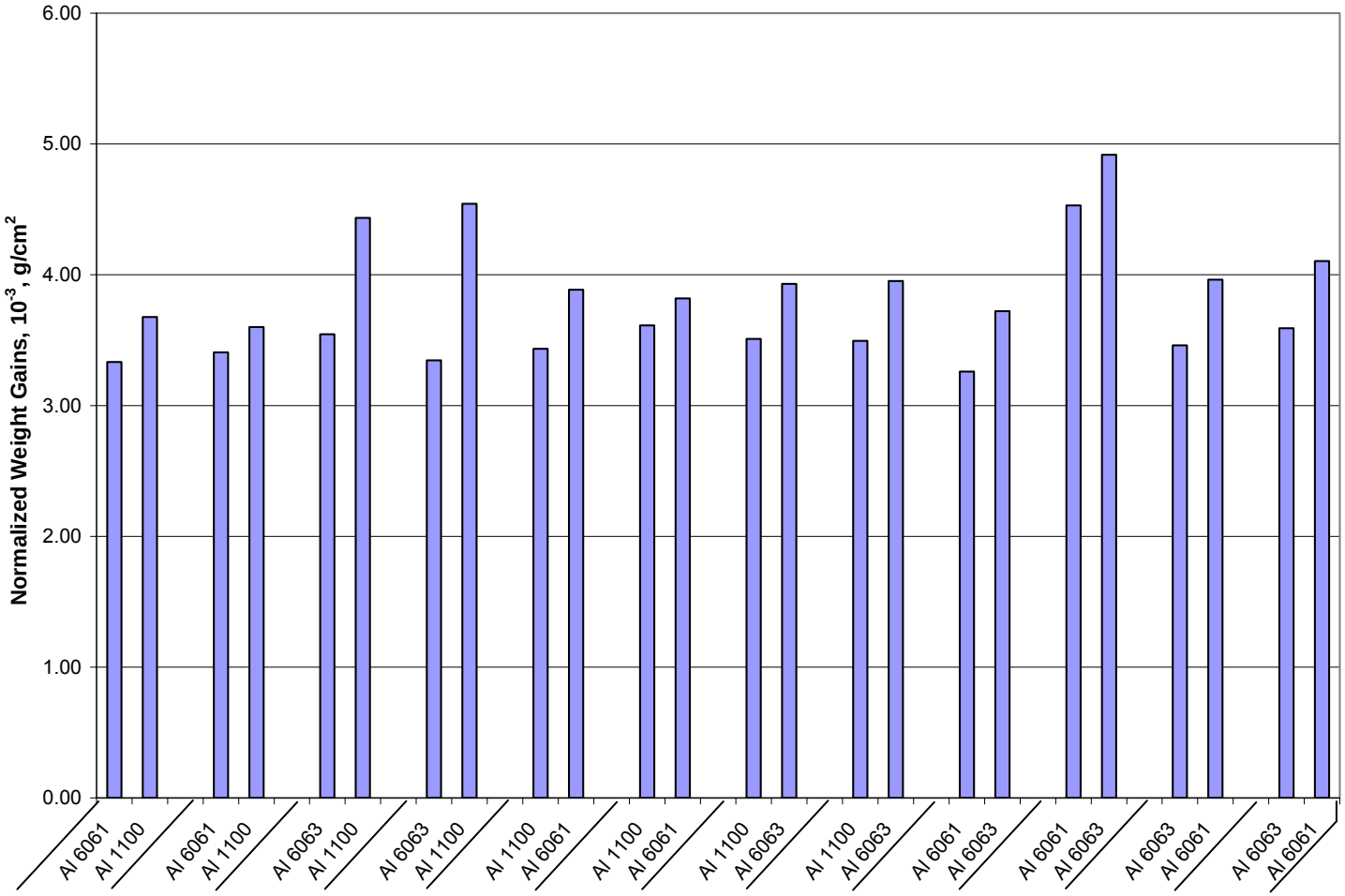

Figure 12. Effect of normalized weight gains from galvanically coupled coupons after 97 months in L-Basin. Note the first alloy listed is the largest coupon (70 mm diameter); the second is the smallest coupon (32 mm diameter). Weight gains were normalized by dividing by the exposed area of the coupon. In all cases, the smaller coupon displayed a higher percentage weight gain than the larger coupon, regardless of the alloy.

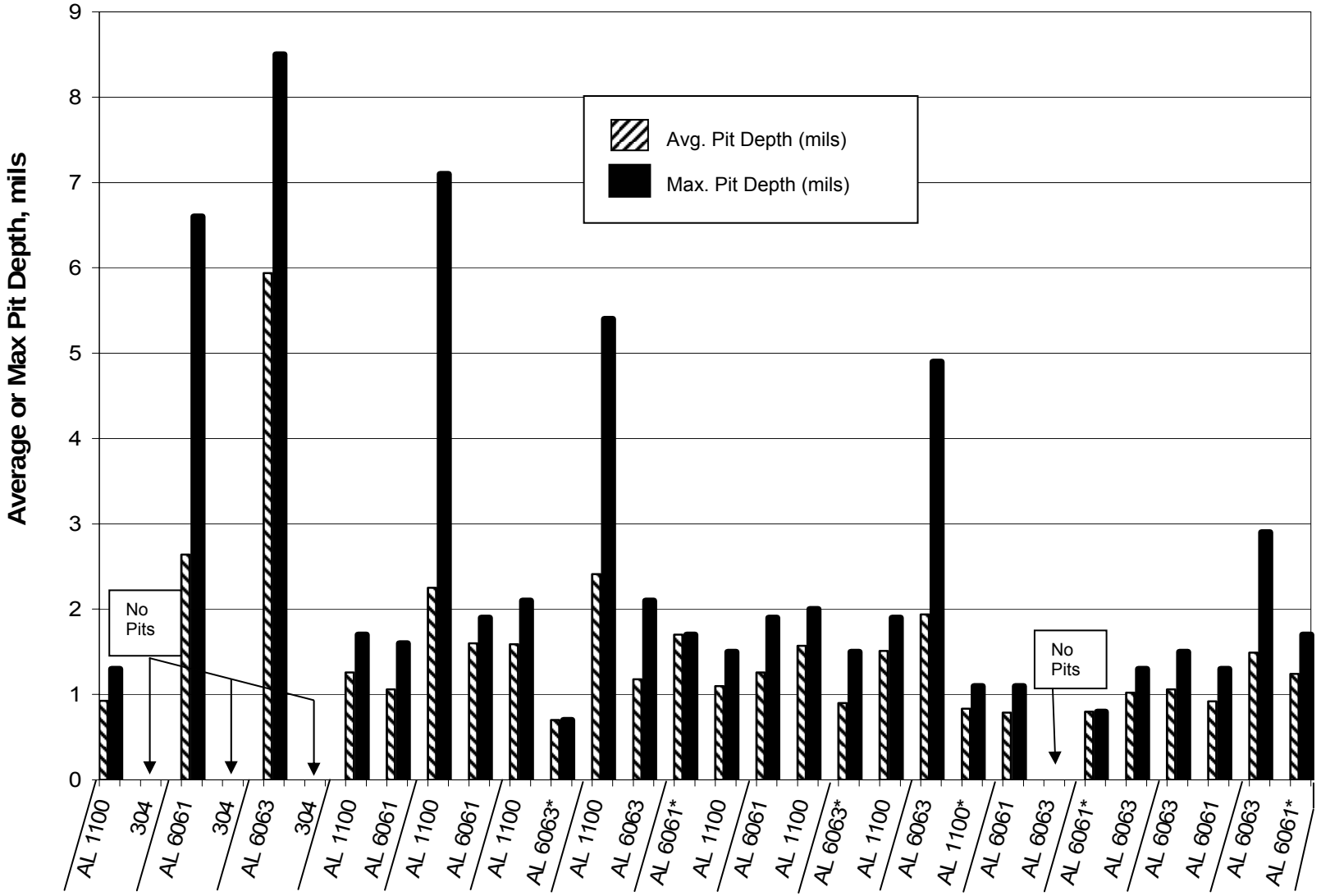

Figure 13. Average and maximum pit depths of 2004 galvanically coupled coupons. Starting at left, the first coupon (group of two) is the smallest (32 mm OD), while the second mating coupon is the largest (70 mm OD). The first three bar sets are coupons mated to 304 stainless steel while the remainder of the coupon sets mate two aluminum alloys together. Maximum pit depths were measured near the edge of the PTFE washer area or at the coupon ID. On samples noted by an asterisk (*), pit depth averages were calculated with <10 pits. No pitting was observed on all 304 and one of the 6063 coupons mated to 6061.

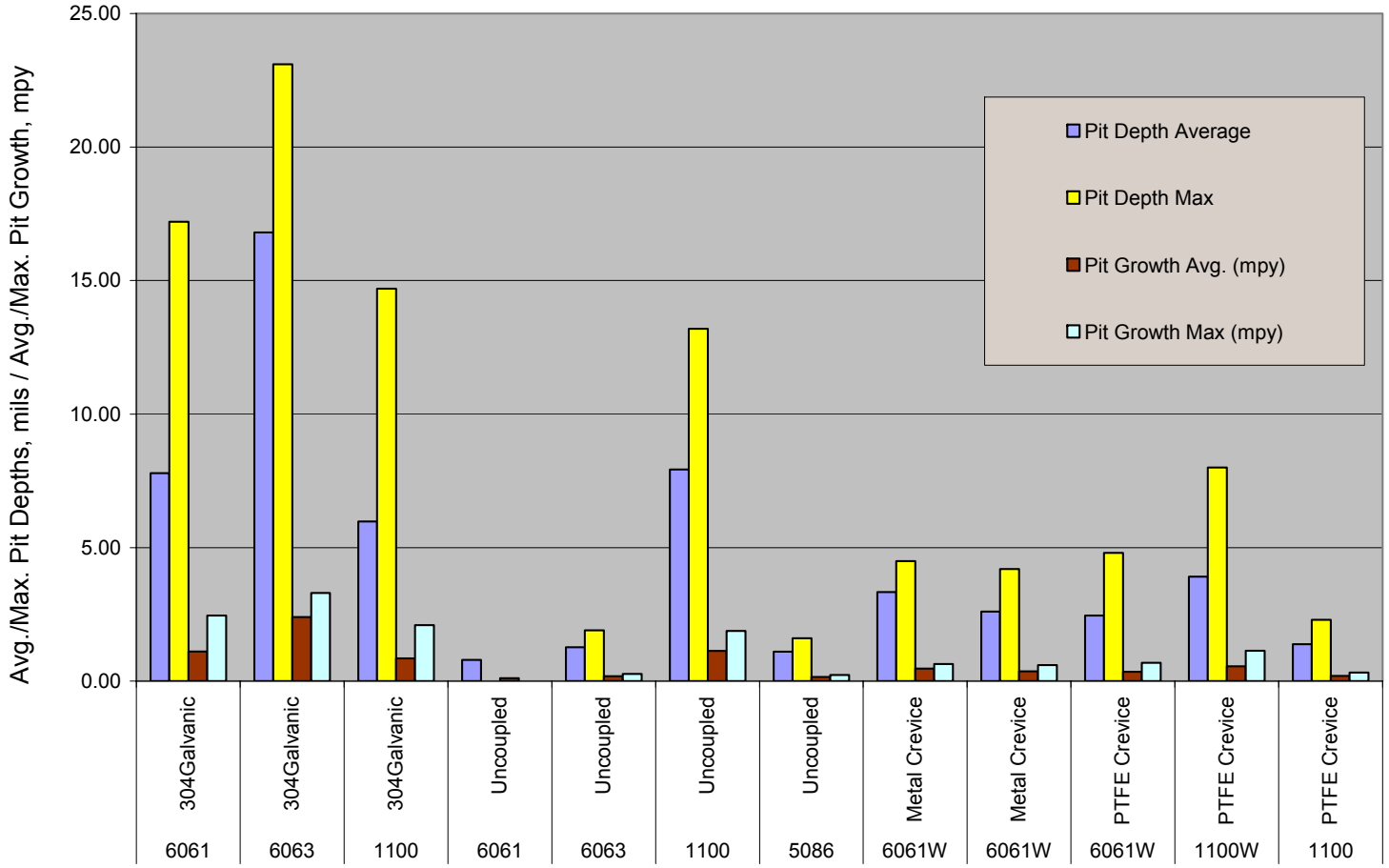

Figure 14. Effect of coupon type and aluminum alloy on pit depths on 2003 coupons. The average and maximum pit depth and the pit growth rate were highest in the 6063/304 couple. As an individual coupon, 1100 revealed greater pit depths than the other three alloys in the uncoupled category.

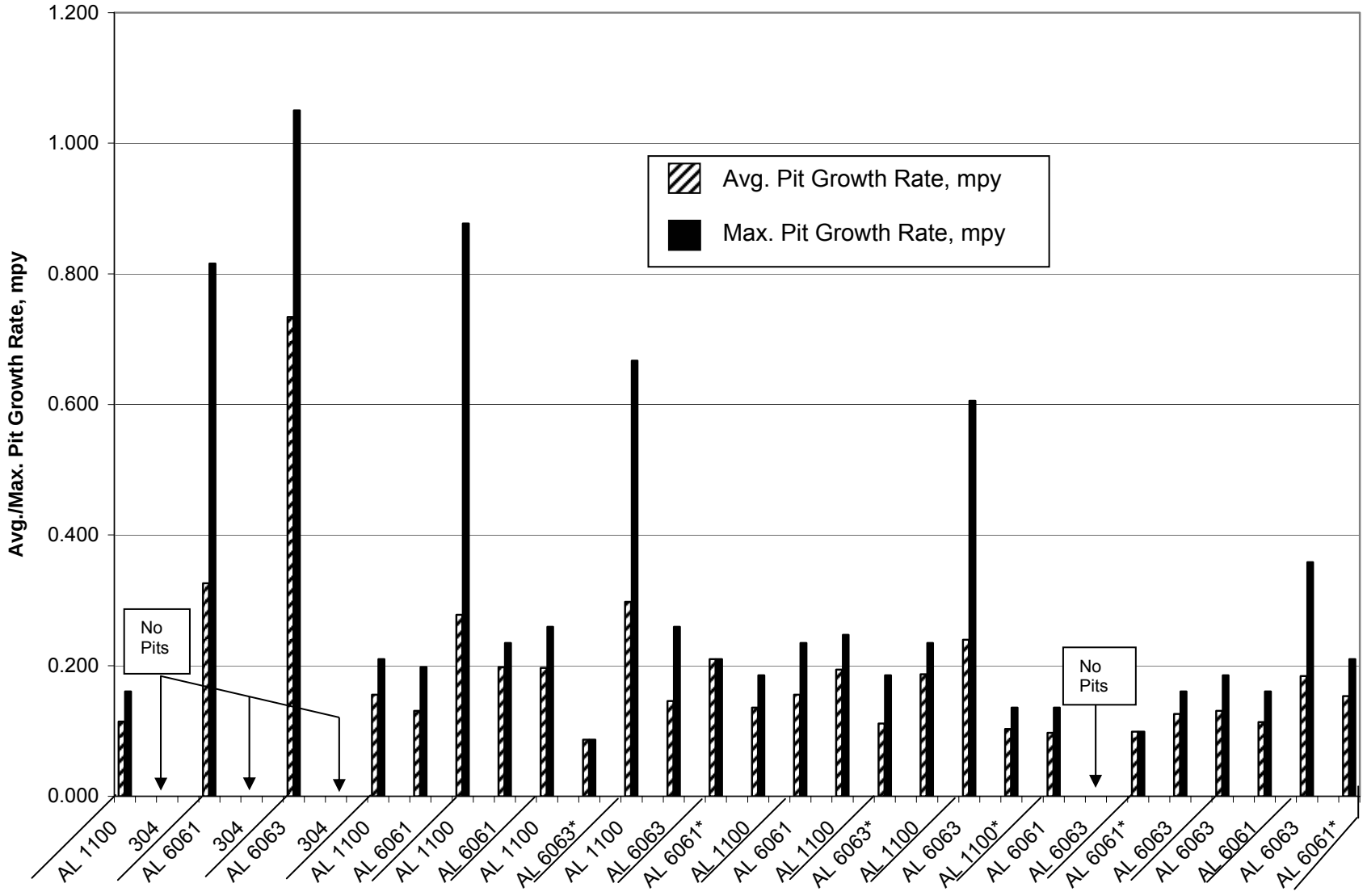

Figure 15. Average and maximum pit growth rates for 2004 galvanically coupled coupons. Coupon order and sizes are identical to those used in Figure 13. The same pit depths were used except divided by the number of years (8+) in the basin to calculate growth rates.

(a) As Received

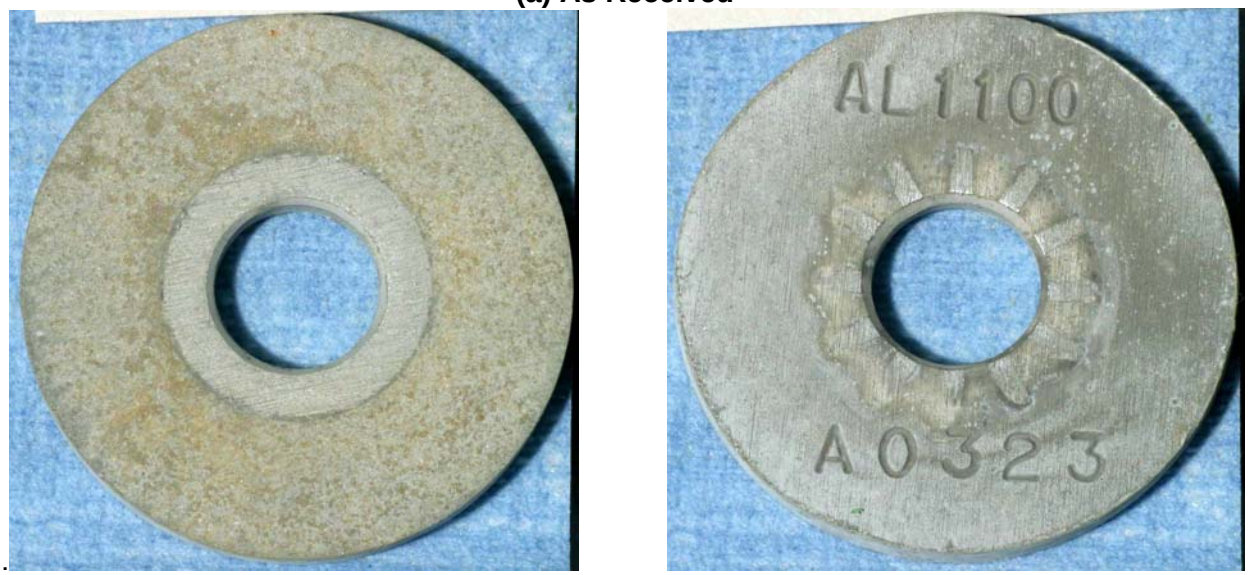

(b) As-Cleaned

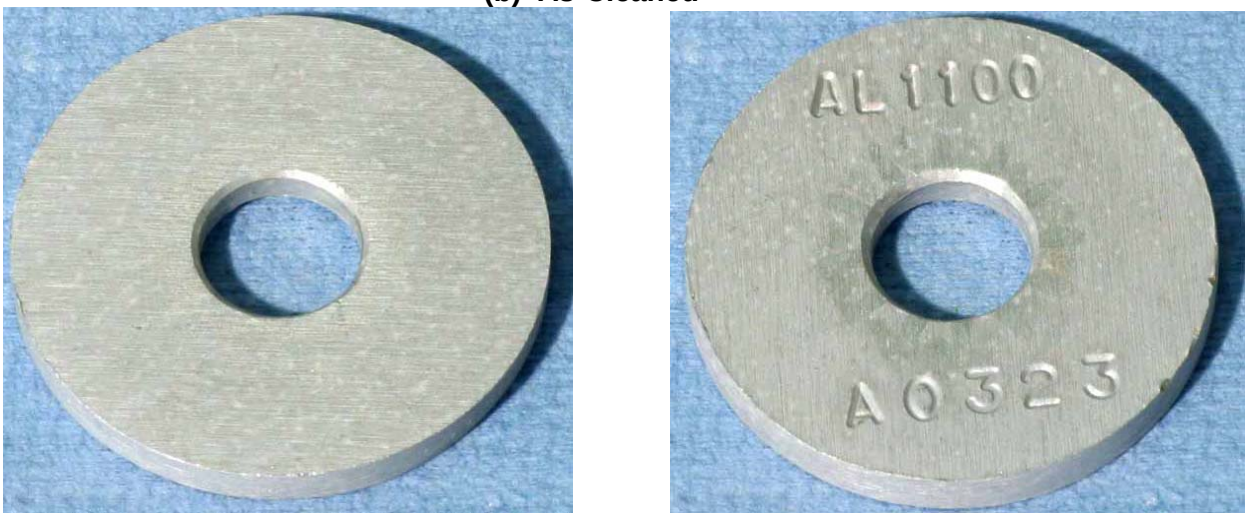

Digital Images

Figure 16. Before and after cleaning imprint of a serrated PTFE washer and its crevice effect on an Al 1100. No pitting was observed within the PTFE washer area.

(a) As-Received

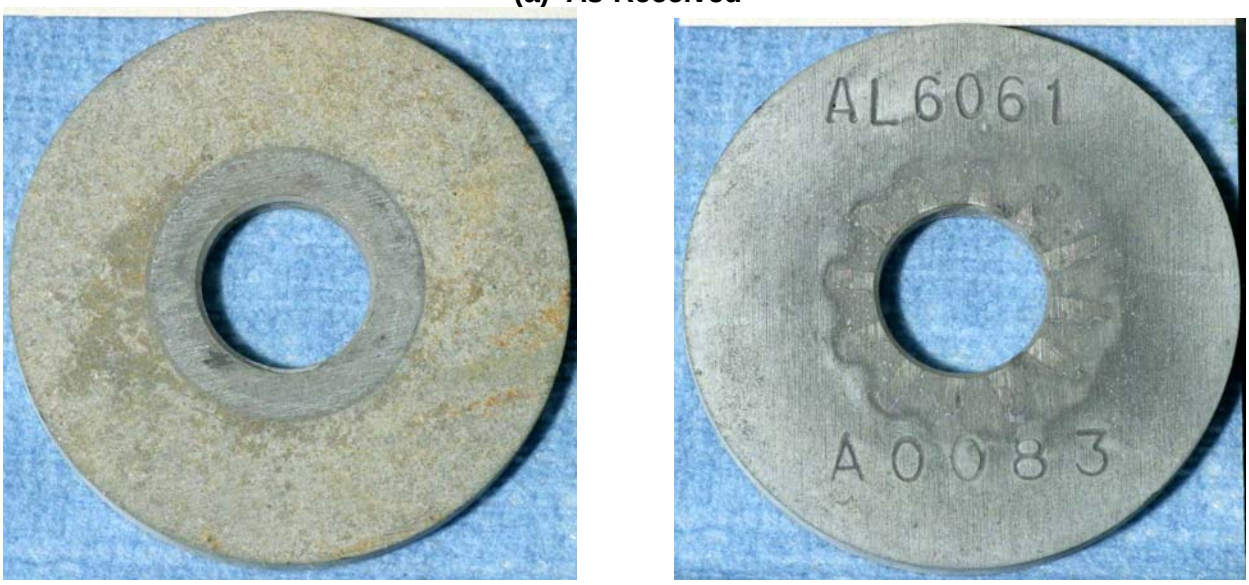

(b) As-Cleaned

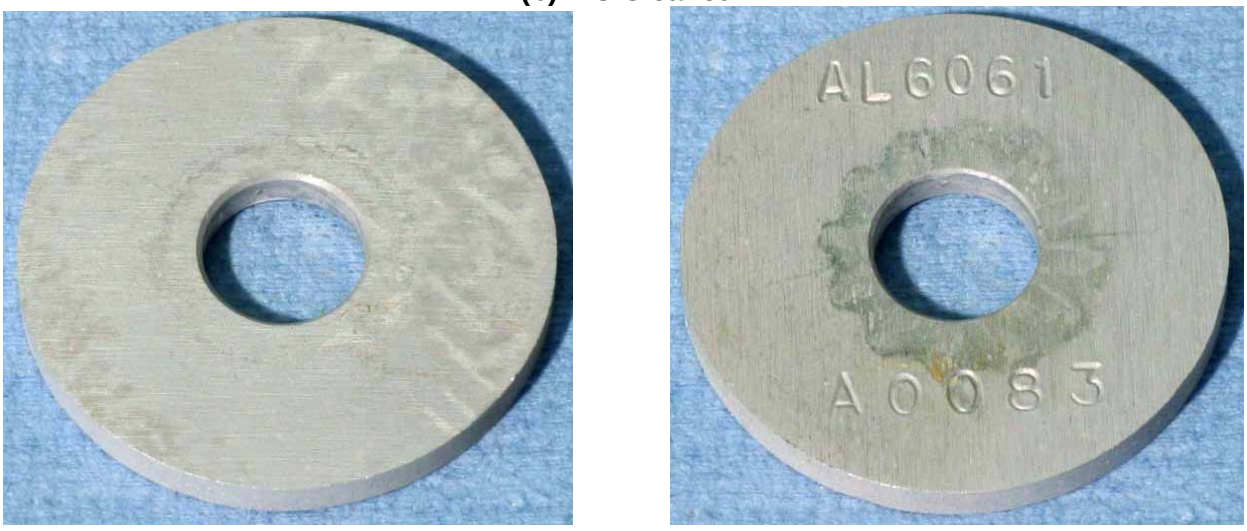

Digital Images

Figure 17. Before and after cleaning imprint of a serrated PTFE washer and its crevice effect on an Al 6061 coupon.

(a) As-received

(b) As-cleaned

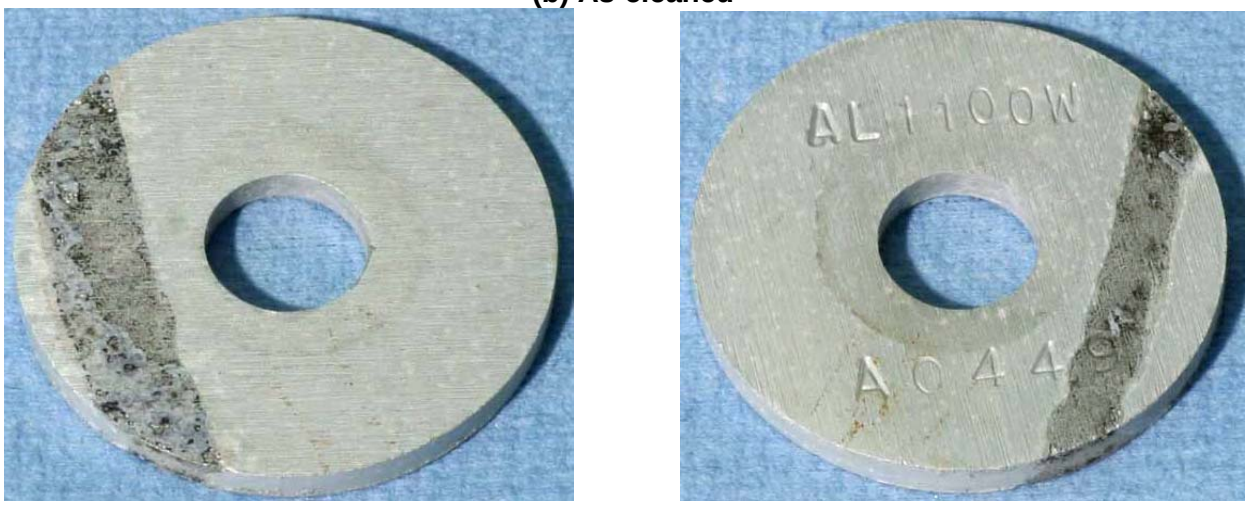

Digital Images

Figure 18. Visual appearance of as-received and as-cleaned autogeneous welded 1100 coupon displaying some retention of black oxide after nitric acid cleaning. Upper left image reveals oxide peeling off when PTFE washer was removed.

(a) As-received

(b) As-cleaned

Digital Images

Figure 19. Visual appearance of as-received and as-cleaned autogeneous welded 6061 coupon displaying some retention of oxide (black) after nitric acid cleaning. Black spots in the weld and in the crevice area left by the PTFE washer indicate possible pit locations.

(a) As-Received

(b) As-Cleaned

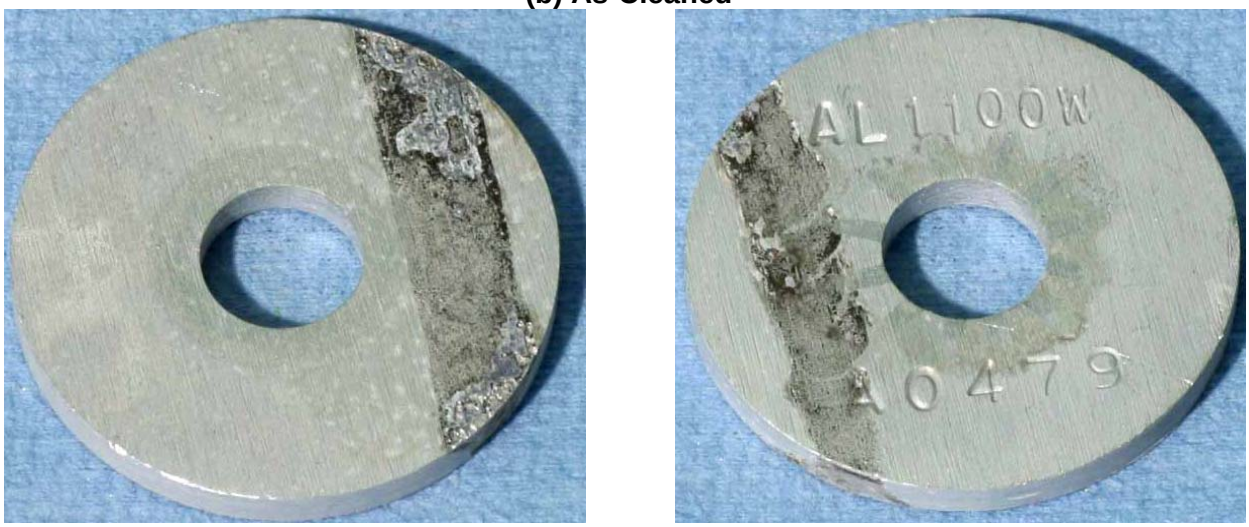

Digital Images

Figure 20. Visual effects of a serrated (crevice) PTFE washer on autogeneous welded 1100W coupon in the as-received and as-cleaned condition. Notice that oxide is still remaining on the lower left image. Limited attempts were made to remove the oxides but extensive pitting was still found in the weld area on both sides (~60 pits in weld on lower left photo and ~40 pits in weld on lower right photo).

(a) As-Received

(B) As-Cleaned

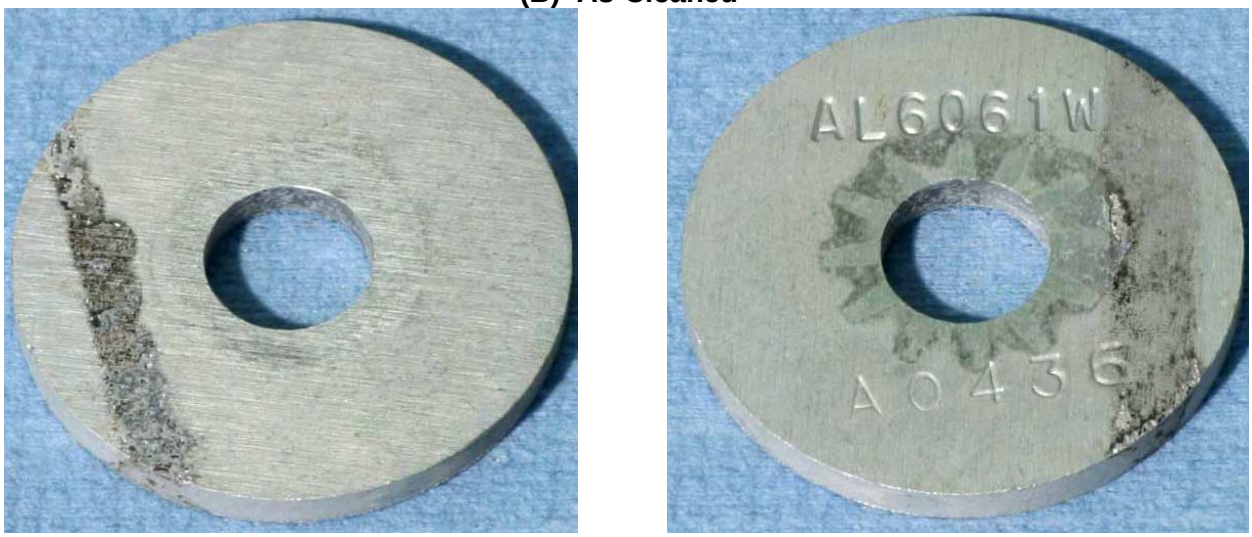

Digital Images

Figure 21. Effect of serrated (crevice) PTFE washer on the visual appearance of as-received and as-cleaned autogeneous welded 6061 coupon.

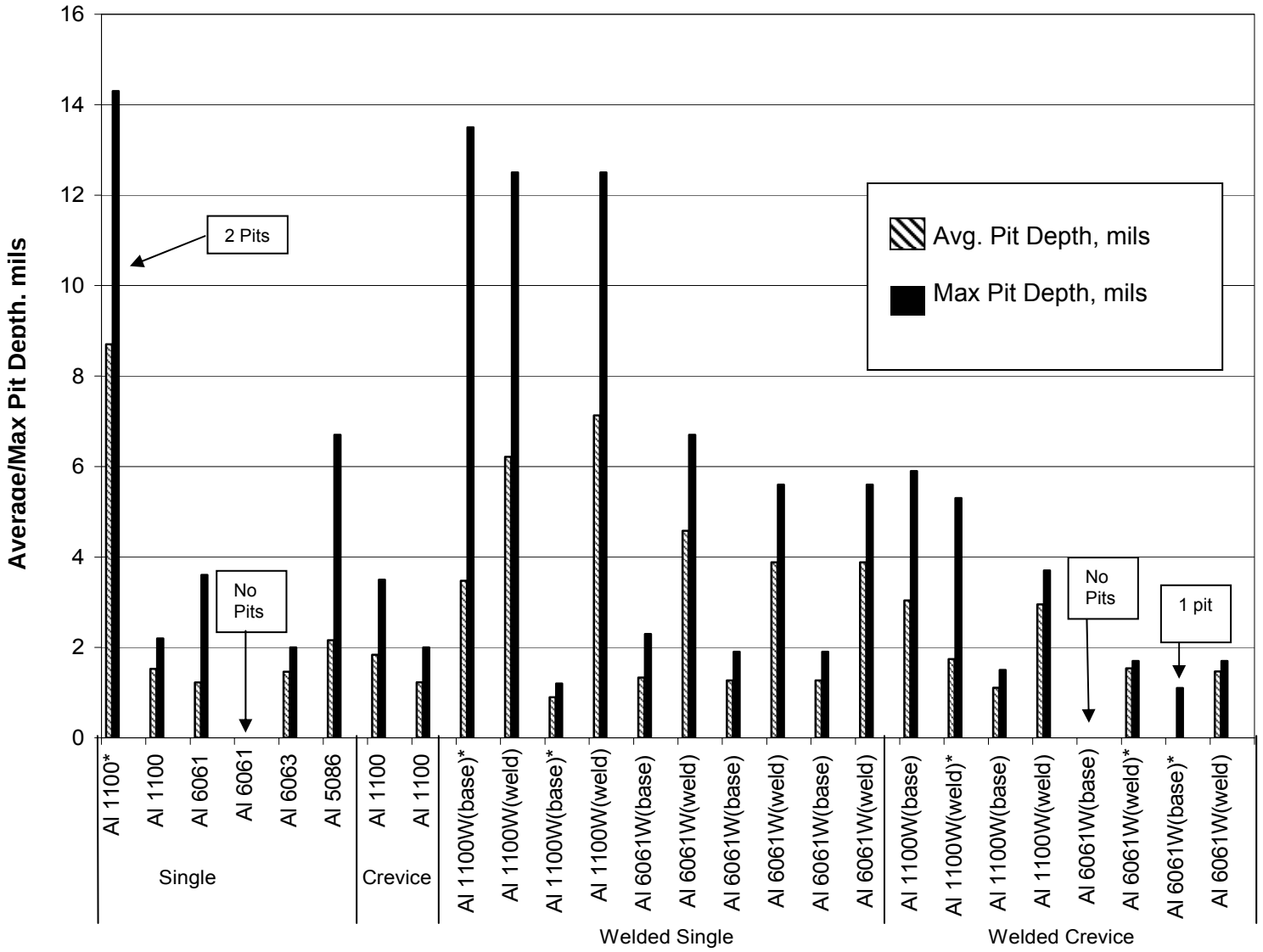

Figure 22. Effect of single, crevice and autogenous welded 2004 coupons (with and without crevice) on average pit depths and maximum pit depths. On samples noted by an asterisk (*), pit depth averages were calculated with <10 pits. The single Al 1100* coupon data is based on two pits. Pits measured in the "base" are those outside of the weld.

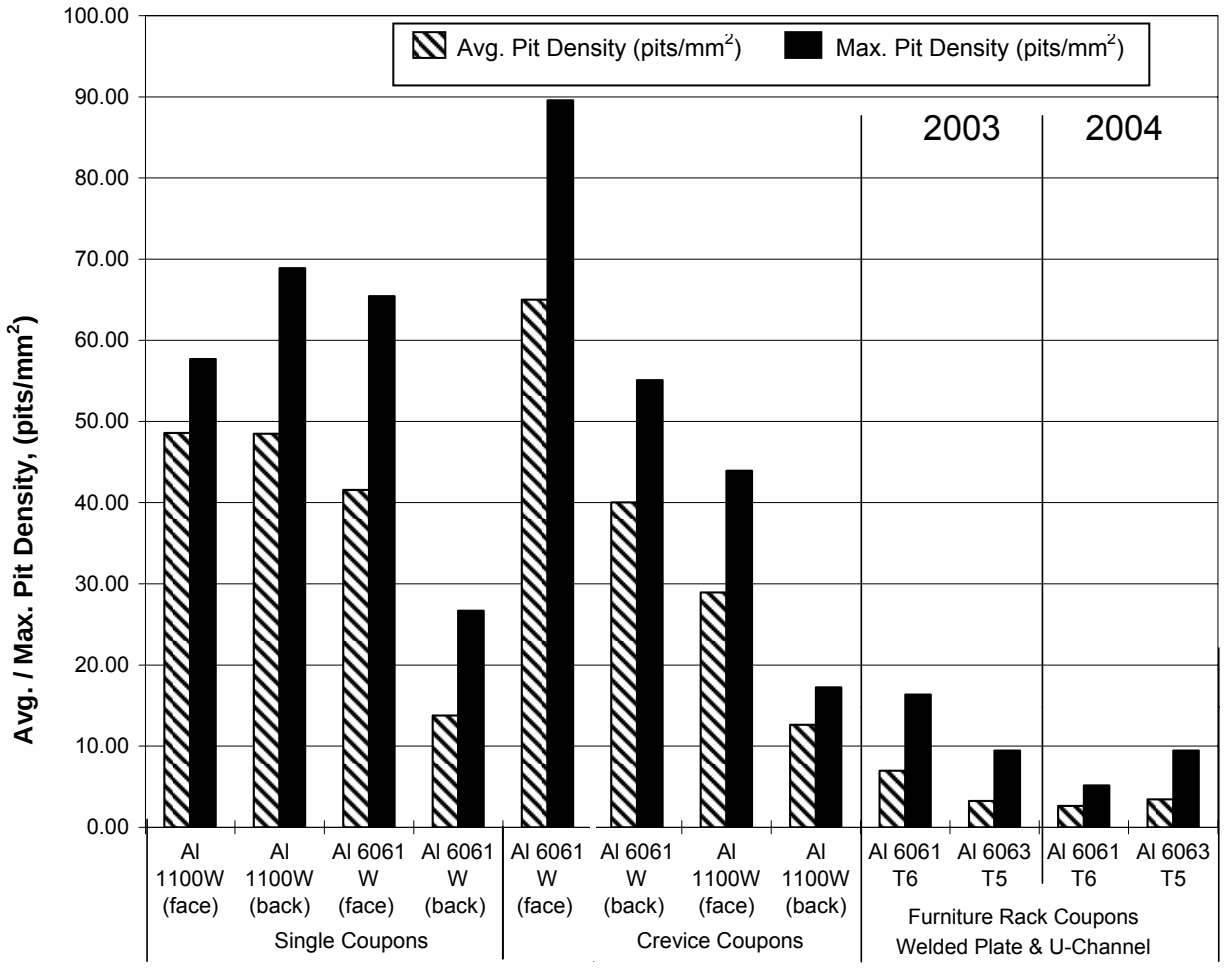

Figure 23. Effect of welded coupon type on average and maximum pit densities. Coupons are individual (welded), crevice (welded), and furniture rack welded (plate and U- channel). The alloy designations including "face" is the side of the coupon with alloy designation and coupon number while the coupon "back" is the opposite side. Furniture rack coupons were welded with a R4043 rod versus autogenous welding of the individual and crevice coupons. Furniture rack coupon revealed the lowest pit densities of all welded coupons.

Digital Image

Figure 24. Aluminum rack furniture samples, with and without welds, after 97 months immersion. Corrosion is visible as the white oxide formation in the heat affected zone of the welds which is similar to that shown in previous years. Plate coupons are 6061-T6 and "U" channel coupons are 6063-T5. Welding was performed with a R4043 filler metal.

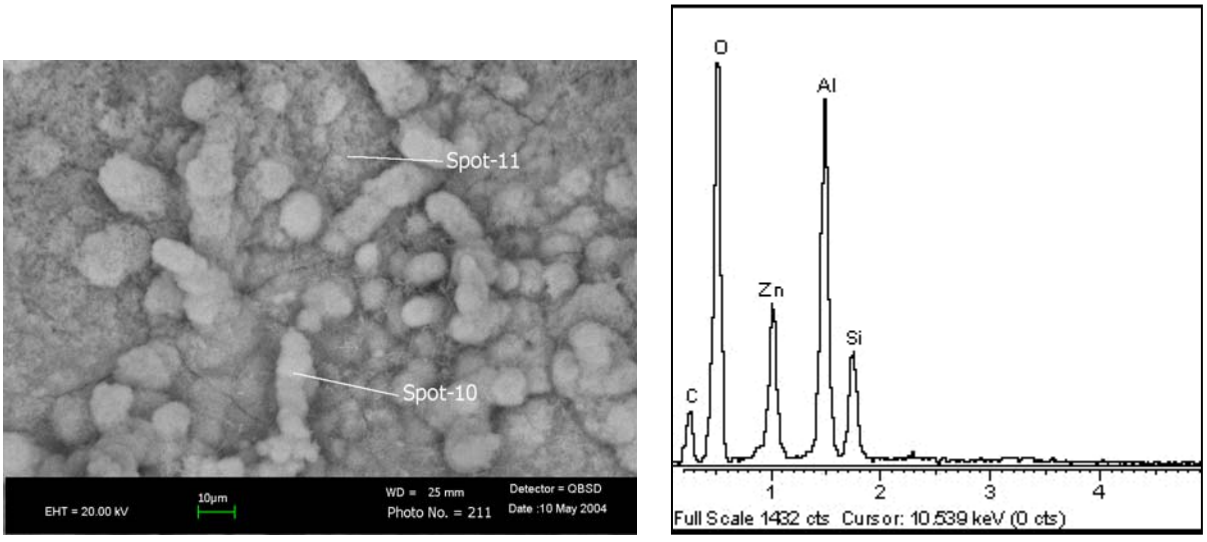

Figure 25. Left photo reveals rod-like morphology in aluminum oxide in HAZ of weld on 6063 T5 U-channel versus particle morphology in base metal oxide. Energy Dispersive Spectroscopy (EDS) of Spot-10 in right graph reveals Zn in rod-like particle along with Al, O, and Si.

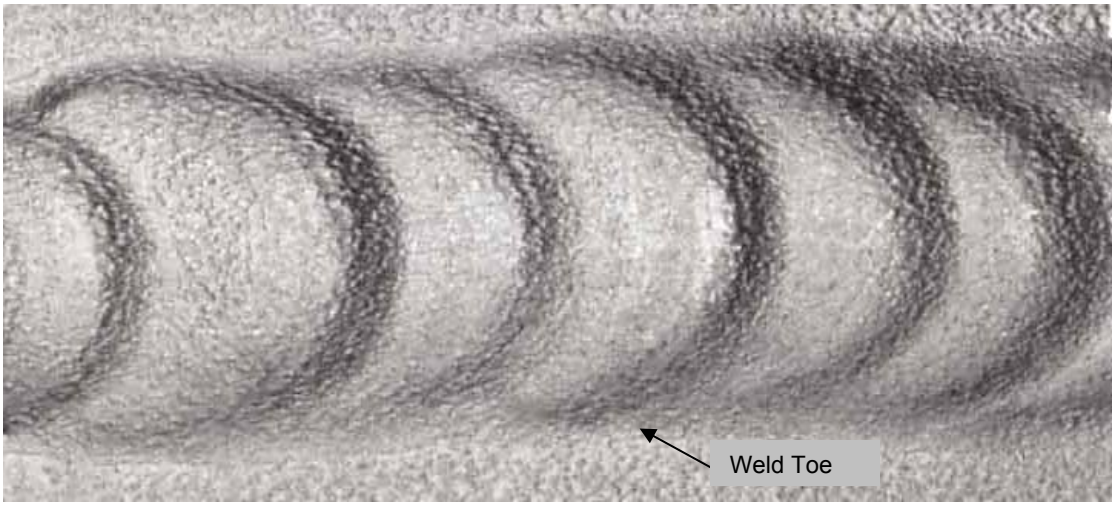

Digital Image

Figure 26. R4043 weld bead on as-received 6063 U-Channel coupon. The welded face of the coupon was either chemically etched or bead blasted to clean the surface after welding. Although the surface of the weld reveals an “orange peel” type surface, no pitting is visible in the weld toe or in the weld face.

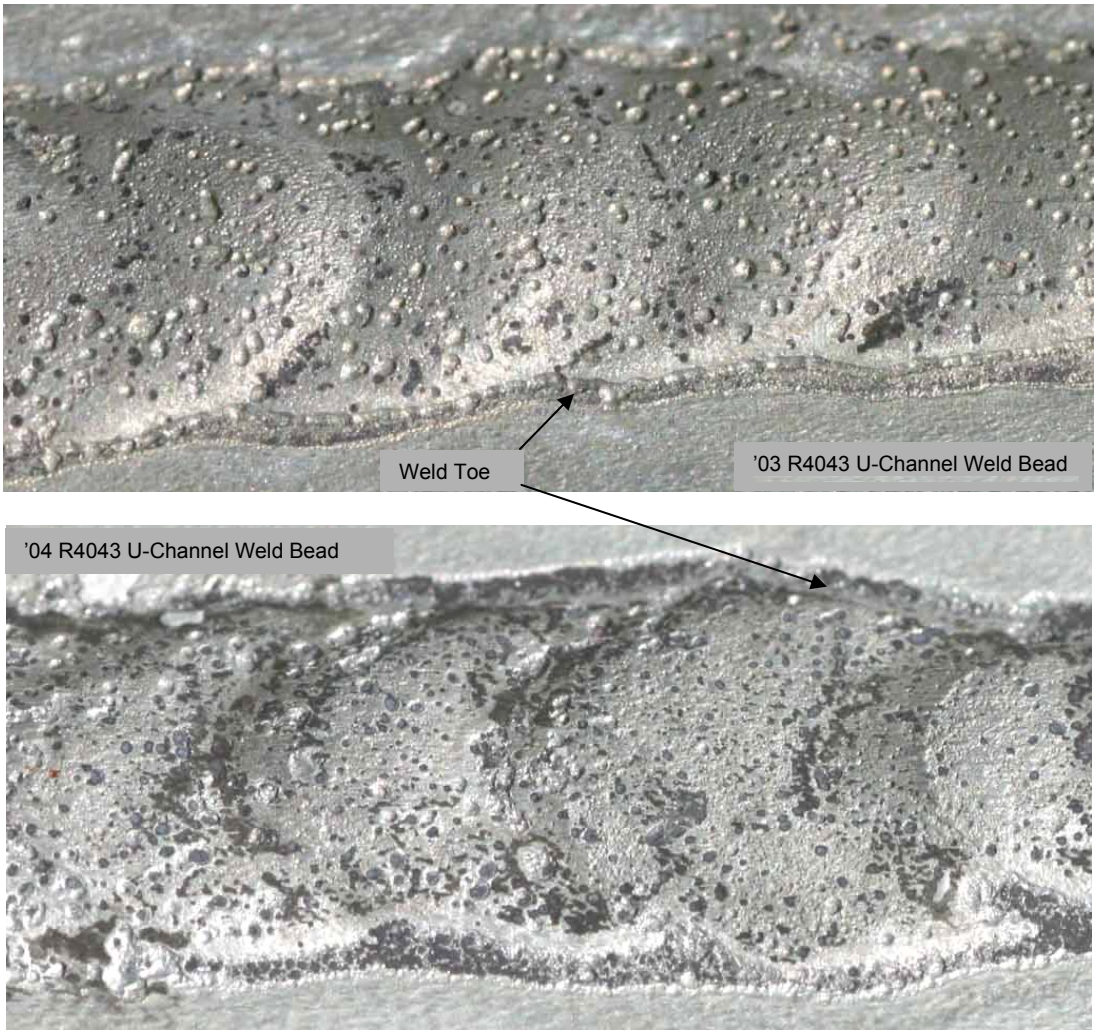

Digital Images

Figure 27. Cleaned R4043 weld beads on 2003 (a) and 2004 (b) 6063 T5 U-Channel samples after immersion in L-Basin for 85 and 97 months, respectively. Vertical width of each weld bead is approximately 6.4 mm. Numerous pits are visible in the weld bead and in the weld toe on each side of the weld bead. Only a few pits were found in the base metal.

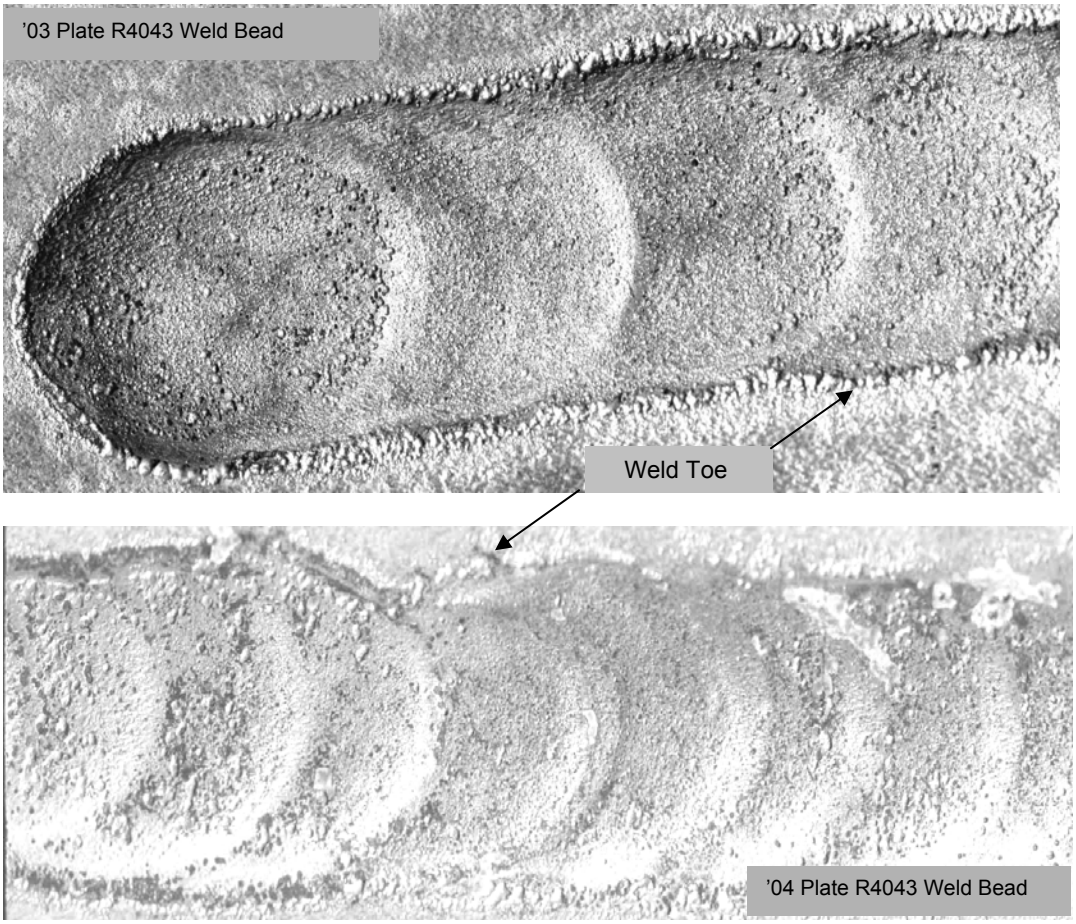

Digital Images

Figure 28. Cleaned R4043 weld beads from '03 and '04 6061 T6 furniture plate samples. Vertical width of weld beads ranges from 6.4 to 9.5 mm. While the number of pits appears to be less than that of the U-channel samples, numerous pits were counted in the weld toe.

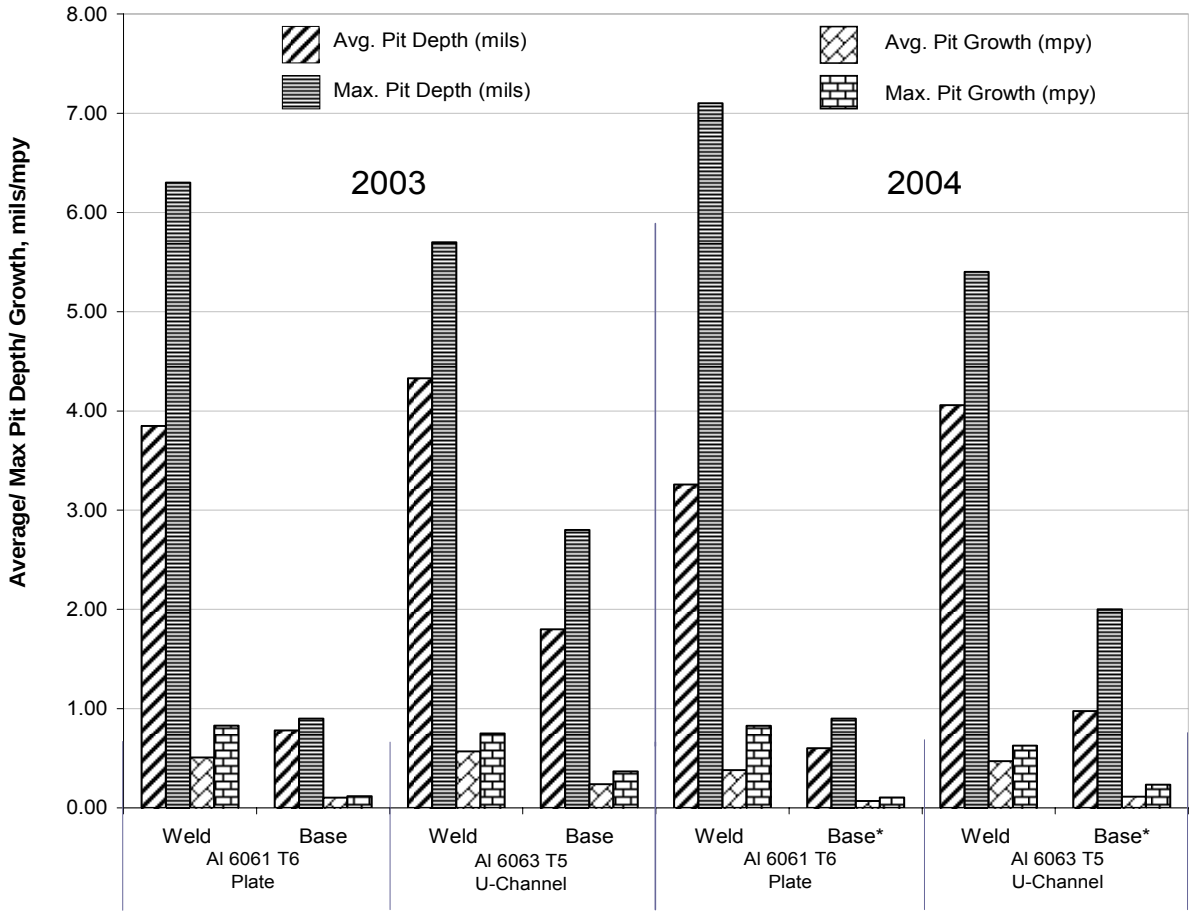

Figure 29. Effect of weld and base metal of furniture rack samples on average (Avg.) and maximum (Max.) pit depths and pit growth rates. Maximum pit depths in the welds were measured in the toe of the weld, while the highest pit densities were in the welds. Growth rates were less than 1 mpy. On samples noted by an asterisk (*), pit depth averages were calculated with <10 pits.

WSRC INTERNAL DISTRIBUTION

D. B. Rose, 704-28L
T. J. Spieker, 704-30L
D. L. Melvin, 704-25L
R. W. Deible, 704-26L
S. C. Declue, 704-K
N. C. Iyer, 773-41A
R. L. Sindelar, 773-41A
J. I. Mickalonis, 773-A
P. R. Vormelker, 773-41A
A. J. Duncan, 773-A
T. H. Murphy, 773-A
D. W. Vinson, 773-41A
M. K. Hicks, 773-41A
SRTC Records, 773-52A